Wnt ligands regulate the asymmetric divisions of neuronal progenitors in C. elegans embryos

Shilpa Kaur, Pauline Mélénec, Sabrina Murgan, Guillaume Bordet, Pierre Recouvreux, Pierre-François Lenne, Vincent Bertrand

Wnt ligands regulate the asymmetric divisions of neuronal progenitors in *C. elegans* embryos

Running Title: Wnt in neuronal divisions

Shilpa Kaur[1], Pauline Mélénec[1], Sabrina Murgan[1], Guillaume Bordet[1], Pierre Recouvreux[1], Pierre-François Lenne[1] and Vincent Bertrand[1,*]

1 Aix Marseille Univ, CNRS, IBDM, Turing Center for Living Systems, Marseille, France

* corresponding author: Vincent Bertrand, vincent.bertrand@univ-amu.fr

KEYWORDS

C. elegans, neuron, asymmetric division, polarity, Wnt signaling

ABSTRACT

Wnt/β-catenin signaling has been implicated in the terminal asymmetric divisions of neuronal progenitors in vertebrates and invertebrates. However, the role of Wnt ligands in this process remains poorly characterized. Here we used the terminal divisions of the embryonic neuronal progenitors in *C. elegans* to characterize the role of Wnt ligands during this process focusing on a lineage that produces the cholinergic interneuron AIY. We observed that during interphase the neuronal progenitor is elongated along the anteroposterior axis, then divides along its major axis, generating an anterior and a posterior daughter with different fates. Using time-controlled perturbations, we show that three Wnt ligands, which are transcribed at higher levels at the posterior of the embryo, regulate the orientation of the neuronal progenitor and its asymmetric division. We also identified a role for a Wnt receptor (MOM-5) and a cortical transducer APC (APR-1), which are respectively enriched at the posterior and anterior poles of the neuronal progenitor. Our study establishes a role for Wnt ligands in the regulation of the shape and terminal asymmetric divisions of neuronal progenitors, and identifies downstream components.

INTRODUCTION

The nervous system of animals is composed of a high diversity of neuronal subtypes. In vertebrates and invertebrates, neurons are often generated by asymmetric divisions of progenitor cells, such as neural stem cells (reviewed in Gotz and Huttner, 2005; Hartenstein and Stollewerk, 2015). Neural stem cells can divide asymmetrically to produce a daughter cell that retains a stem cell fate while the other daughter differentiates into a neuron or acquires a more restricted progenitor fate. In addition, neuronal progenitors can divide asymmetrically to produce two neurons with different identities. Several pathways have been implicated in the control of these terminal asymmetric divisions. In vertebrates and *C. elegans*, the Wnt pathway plays a role in the regulation of neuronal progenitor asymmetric divisions (reviewed in Bertrand, 2016; Bielen and Houart, 2014). For example, in the mouse cortex, it has been observed that the Wnt pathway regulates the generation of neurons from neural stem cells (Woodhead et al., 2006; Zhang et al., 2010) and the asymmetry of neural stem cell divisions (Delaunay et al., 2014). However, the precise role played in this process by endogenous Wnt ligands (secreted activator of the Wnt pathway) *in vivo* remains to be determined. In mammals, this task is complicated by the presence of 19 different Wnt ligands in the genome (Nusse and Clevers, 2017). *C. elegans*, with only 5 Wnt ligands, is a simpler model organism to address this question (Sawa and Korswagen, 2013).

In *C. elegans*, most neurons are born during embryonic development at the stage of neurulation (termed epidermal enclosure in *C. elegans*). At this stage, the ventral surface of the embryo is covered by neuronal progenitors (Fig. 1A, each green dot represents the nucleus of a neuronal progenitor). Each neuronal progenitor divides asymmetrically along the anteroposterior axis to generate two postmitotic daughter cells that usually differentiate into two neurons with different identities (Sulston et al., 1983). We have previously shown that the terminal asymmetric divisions of embryonic neuronal progenitors are regulated by a particular Wnt pathway termed the Wnt/β-catenin asymmetry pathway (Bertrand and Hobert, 2009). This pathway regulates several asymmetric divisions during *C. elegans* embryonic and postembryonic development (Bertrand, 2016; Kaletta et al., 1997; Phillips and

Kimble, 2009; Sawa and Korswagen, 2013). Whether Wnt ligands regulate the terminal asymmetric divisions of neuronal progenitors in the embryo remains to be determined.

To analyze the role of Wnt ligands in the terminal asymmetric divisions of neuronal progenitors, we focused on a specific test lineage, the AIY lineage, that is well characterized and for which many tools are available. AIY is a cholinergic interneuron that is generated by asymmetric division in the embryo. During neurulation the AIY mother cell divides asymmetrically to generate a posterior daughter that differentiates into the AIY interneuron, and an anterior daughter that differentiates into a cholinergic motor neuron, SMDD (Fig. 1B). There are two AIY lineages, left and right, located on the left and right sides of the midline respectively (Fig. 1A). During neurulation, the two SMDD/AIY mother cells are located on the ventral side of the embryo in the middle of the field of neuronal progenitors (Fig. 1A). Using time-controlled perturbations of intracellular components of the Wnt pathway, we have previously identified the Wnt/β-catenin asymmetry pathway as a key regulator of the terminal asymmetric division of the SMDD/AIY mother (Bertrand and Hobert, 2009). Before terminal division, the expression of the LIM-homeodomain transcription factor TTX-3 (a LHX2/9 ortholog) is initiated in the SMDD/AIY mother (Bertrand et al., 2011; Bertrand and Hobert, 2009; Murgan et al., 2015) (Fig. 1B). Following cell division, the TTX-3 protein is inherited in the two daughters, the SMDD and AIY neurons. In the posterior daughter (AIY), the intracellular Wnt pathway is active leading to the accumulation of the β-catenin SYS-1 and the reduction of the nuclear concentration of the TCF transcription factor POP-1 (Bertrand and Hobert, 2009). As a consequence, the majority of the nuclear POP-1 proteins are bound to SYS-1 forming a complex that activates transcription allowing the maintenance of TTX-3 expression in AIY following division (Bertrand and Hobert, 2009). TTX-3 then activates and maintains the expression of a large battery of terminal differentiation genes (neurotransmitter receptors, ion channels, *etc.*) responsible for the specific functions of the AIY neurons (Bertrand and Hobert, 2009; Wenick and Hobert, 2004). In the anterior daughter cell (SMDD), the intracellular Wnt pathway is inactive, the β-catenin SYS-1 does not accumulate, POP-1/TCF nuclear concentration is high, and POP-1/TCF free of SYS-1/β-catenin, acts as a repressor (Bertrand and Hobert, 2009).

TTX-3 expression is therefore not maintained disappearing from the SMDD neuron before hatching (Bertrand and Hobert, 2009). While intracellular components of the Wnt pathway, such as POP-1/TCF and SYS-1/β-catenin, are clearly involved in the regulation of the SMDD/AIY mother asymmetric division, whether extracellular Wnt ligands and their transmembrane receptors also play a role remains to be determined.

In this study, we observe that three Wnt ligands (CWN-1, CWN-2 and MOM-2) are expressed in the embryo during neurulation. They are transcribed at a higher level in the posterior region than in the anterior region. Using time-controlled loss- and gain-of-function approaches coupled with *in vivo* quantitative imaging, we show that these Wnt ligands play a redundant role in the regulation of the SMDD/AIY mother asymmetric division. The mother cell is elongated along the anteroposterior axis before division and the Wnt ligands regulate the orientation of this elongation. They also control the orientation of the division and the asymmetry of daughter cell fates. This process involves a transmembrane receptor of the frizzled family (MOM-5) that is transiently enriched at the posterior pole of the mother cell, and a cortical protein of the APC family (APR-1) that is enriched at the anterior pole of the mother cell and is preferentially inherited by the anterior daughter. Therefore, this study identifies a role for Wnt ligands in the regulation of the orientation of embryonic neuronal progenitors and in the control of their terminal asymmetric divisions.

RESULTS

The SMDD/AIY neuronal progenitor is elongated along the anteroposterior axis before its division.

The *ttx-3* gene is expressed in the SMDD/AIY mother cell before its terminal asymmetric division (Bertrand and Hobert, 2009). We therefore used a transgenic line expressing a cytoplasmic GFP under the control of the *ttx-3 cis*-regulatory elements to determine whether the SMDD/AIY mother displays any sign of morphological asymmetry before its division. Interestingly, we observed that the SMDD/AIY mother is elongated along the anteroposterior axis before division (Fig. 1C). We quantified the elongation factor and its orientation over time using time-lapse imaging. After fitting the cell with an ellipse, we defined the elongation factor as the ratio between the major and minor axis of the ellipse. The orientation of the cell is then determined as the angle between its major axis and the anteroposterior axis of the embryo (Fig. 1D, E). The SMDD/AIY mother appears already elongated when the GFP signal starts being detectable (around 30 minutes before division) (Fig. 1D). The elongation factor then remains constant until a few minutes before division when the cell becomes rounded during mitosis. In addition, we observed that the orientation of the SMDD/AIY mother is largely biased toward the anteroposterior axis before division (Fig. 1E). Therefore, the SMDD/AIY mother is morphologically polarized along the anteroposterior axis before its division. Subsequently, the SMDD/AIY mother divides along the anteroposterior axis generating the SMDD motor neuron anteriorly and the AIY interneuron posteriorly (Fig. 1C, 1E).

The Wnt ligands CWN-1, CWN-2 and MOM-2 regulate the asymmetric division of the SMDD/AIY neuronal progenitor.

We have previously determined that, following asymmetric division of the SMDD/AIY mother cell, a complex between the transcription factor POP-1/TCF and its coactivator SYS-1/β-catenin forms in the nucleus of the posterior daughter AIY but not of the anterior daughter SMDD, leading to the acquisition of different fates by AIY

and SMDD (Bertrand and Hobert, 2009). However, how this asymmetry in the Wnt pathway is initially established is unknown. We therefore analyzed whether Wnt ligands, which are secreted activators of the Wnt pathway, could be involved in the polarization of the SMDD/AIY mother division. There are 5 Wnt ligands in the *C. elegans* genome (Sawa and Korswagen, 2013). Using transcriptional reporters of the 5 Wnt ligands (*cis*-regulatory elements of the Wnt ligands placed upstream of a nuclear GFP (Gleason et al., 2006)), we observed that 3 Wnt ligands (CWN-1, CWN-2 and MOM-2) are expressed in the embryo at the time of the terminal division of the SMDD/AIY mother cell (Fig. 2A). We could not detect expression of the two remaining Wnt ligands (LIN-44 and EGL-20) at that time (Fig. 2A) but start seeing expression at later stages, during elongation, in the posterior end of the embryo. Interestingly, at the time of the terminal division of the SMDD/AIY mother cell, *cwn-1*, *cwn-2* and *mom-2* are transcribed at a higher level in the posterior region of the embryo than in the anterior region (Fig. 2A). These observations are consistent with an analysis of the transcription pattern of Wnt ligands by fluorescent *in situ* hybridization (Harterink et al., 2011). *cwn-1*, *cwn-2* and *mom-2* are transcribed in serveral tissues: *cwn-1* (posterior muscle), *cwn-2* (posterior neuronal progenitors, posterior epidermis, intestine and posterior muscle) and *mom-2* (posterior epidermis and muscle). Their zygotic expression starts during gastrulation and remains during embryonic elongation. To determine the protein localization of these Wnt ligands we tagged them with YFP using a fosmid reporter strategy (see material and methods). Interestingly, the CWN-1::YFP and CWN-2::YFP proteins are detectable in the region where the SMDD/AIY mother cell is present, anterior to their source (Fig. S1). This suggests that CWN-1 and CWN-2 move away from their posterior source to the SMDD/AIY mother area. For MOM-2::YFP the fluorescence levels are too low to conclude.

The correlation between the expression pattern of the Wnt ligands and the asymmetric division of the SMDD/AIY mother cell prompted us to test whether these Wnt ligands regulate this asymmetric division. We first analyzed the effect of loss or gain of function of the three Wnt ligands on the asymmetry of daughter cell fates. Following asymmetric division, the expression of *ttx-3* is maintained in the postmitotic AIY neuron, where it acts as a key determinant of AIY fate, but disappears from the postmitotic SMDD neuron. This restriction of *ttx-3* expression to AIY is regulated by

POP-1/TCF and SYS-1/β-catenin (Bertrand and Hobert, 2009). We first analyzed the effect of two loss-of-function alleles of *cwn-1* and *cwn-2* (*ok546* and *ok895*), which are viable. We observed no clear defect on AIY fate (assessed by *ttx-3* expression) in single mutants of *cwn-1* and *cwn-2*, or in *cwn-1; cwn-2* double mutants (Fig. 2B, left graph). As *mom-2* null mutants are lethal, we used a thermosensitive allele (*ne874ts*) (Nakamura et al., 2005). Embryos were shifted to the restrictive temperature one hour before the division of the SMDD/AIY mother and analyzed at hatching (Fig. 2B, right graph). We observed no defect on AIY fate in single mutants of *mom-2* or in double mutants *mom-2; cwn-1* or *mom-2; cwn-2*. However, in triple *mom-2; cwn-1; cwn-2* mutants, we observed a significant loss of *ttx-3* expression in AIY (Fig. 2B, 2D). This suggests that CWN-1, CWN-2 and MOM-2 play a redundant role in the generation of the AIY neuron. We then tested whether overriding the asymmetry of Wnt ligand expression by strongly and ubiquitously overexpressing one of the Wnt ligands, using a heat shock promoter, would perturb the generation of the AIY neuron. When CWN-2 is ubiquitously overexpressed before the terminal division of the SMDD/AIY mother (that happens at 300 minutes in Sulston timetable (Sulston et al., 1983)), we observed a significant duplication of AIY fate, *ttx-3* becoming ectopically expressed in its sister neuron SMDD (Fig. 2C, 2D). Interestingly, we did not observe this effect when CWN-2 is ubiquitously overexpressed after the terminal division of the SMDD/AIY mother, suggesting that the signal carried by Wnt ligands is read by the mother cell rather than its daughters to generate asymmetric cell fates. Taken together, these data suggest that Wnt ligands regulate the asymmetry of daughter cell fates by signaling to the mother. Loss of Wnt or Wnt ubiquitous overexpression leads to a loss of the asymmetry of daughter cell fates but in opposite directions: conversion of the posterior daughter into an anterior daughter in the loss of function, conversion of the anterior daughter into a posterior daughter in the gain of function. The phenotypes of loss or gain of function of Wnt ligands are only partially penetrant. This could be due to the fact that the Wnt loss or gain of function is only partial or that another cue acts in parallel (see discussion for more details).

Next, we analyzed whether Wnt ligands also regulate the elongation of the SMDD/AIY mother cell and the orientation of its division. In single, double or triple Wnt ligand mutants the elongation factor of the SMDD/AIY mother cell is not affected (Fig. S2A). However, we observed a perturbation of the orientation of the mother cell

in Wnt ligand mutants (Fig. 3A,B). While in single or double Wnt ligand mutants the orientation is not highly perturbed, the cell pointing along the anteroposterior axis, in triple *mom-2; cwn-1; cwn-2* mutants we observed a significant defect, the orientation appearing more random. We also analyzed the effect of Wnt ligand mutants on the orientation of the division of the SMDD/AIY mother cell (Fig. 3C). In Wnt ligand mutants the division appears less strictly oriented along the anteroposterior axis, the defect being higher in the triple *mom-2; cwn-1; cwn-2* mutants. All together, this suggests that Wnt ligands play a redundant role and ensure the correct orientation of the SMDD/AIY mother cell elongation and division along the anteroposterior axis. We then tested whether overriding the asymmetry of Wnt ligand expression by ubiquitously overexpressing CWN-2 would perturb the orientation of the SMDD/AIY mother. Ubiquitous overexpression of CWN-2 does not affect the elongation factor but perturbs the orientation of the cell (Fig. S2A, Fig. 3A,D). The orientation of the division also appears defective following CWN-2 ubiquitous overexpression (Fig. 3E). Taken together, these data indicate that Wnt ligands regulate the orientation of the mother cell, the orientation of its division and the subsequent asymmetry of daughter cell fates.

Our data suggest that Wnt ligands play an instructive role in the regulation of the asymmetric division. To further test this hypothesis, we chose to generate an ectopic lateral source of Wnt and test whether this can reorient the division. We induced a local heat shock using a focused infrared laser (Kamei et al., 2009) in the strain where CWN-2 expression is under control of a heat shock promoter (*hsp::cwn-2*). Induction of CWN-2 expression laterally produces a low penetrance but significant reorientation of the long axis of the SMDD/AIY mother cell towards the medio-lateral axis (Fig. S3, red segments). The division of the SMDD/AIY mother is also reoriented towards the medio-lateral axis. This effect is not observed when CWN-2 expression is induced posteriorly (in its normal site of expression). These results reinforce the idea that the site of Wnt expression is instructive. The weak penetrance of the effect is probably due to the fact that the local transient heat shock is not sufficient to reach high enough levels of CWN-2 expression.

A secreted Wnt antagonist of the SFRP family, SFRP-1, is expressed in the anterior region of the embryo at the time of the terminal divisions of neuronal

progenitors (Harterink et al., 2011). We therefore analyzed the effect of a null allele of *sfrp-1*, *gk554*, on the asymmetric division of the SMDD/AIY mother. We observed no defect of AIY fate (Fig. S4). In addition, no strong effect was observed on the elongation factor of the SMDD/AIY mother, the orientation of this elongation or the orientation of the division (Fig. S2A, Fig. S5). This suggests that SFRP-1, in contrast to the three Wnt ligands, does not play a key role in the asymmetric division of the SMDD/AIY mother.

The Wnt receptor MOM-5 regulates the asymmetric division of the SMDD/AIY neuronal progenitor and is transiently enriched at the posterior pole.

To better understand how Wnt ligands polarize the SMDD/AIY mother we next tried to identify the transmembrane receptors involved in this process. There are six receptors for Wnt in *C. elegans* (Sawa and Korswagen, 2013): four of the Frizzled family (MOM-5, CFZ-2, LIN-17 and MIG-1), one of the ROR family (CAM-1) and one of the RYK family (LIN-18) (Fig. S2B). We analyzed the effect of loss-of-function mutations in each of them (*mom-5(gk812)*, *cfz-2(ok1201)*, *lin-17(n677)*, *mig-1(e1787)*, *cam-1(gm122)*, *lin-18(e620)*). We did not observe any defect in the generation of the AIY neuron in mutants for *cfz-2*, *lin-17*, *mig-1*, *cam-1* and *lin-18* (Fig. S4). However, a loss of AIY identity was observed when *mom-5* was inactivated using the *gk812* mutation or when *mom-5* was knocked down using RNAi (Fig. 4A). In addition, in *mom-5(RNAi)* treated embryos, the SMDD/AIY mother is still elongated (Fig. S2A) but the orientation of the cell is perturbed (Fig. 4B). The orientation of the division is also affected (Fig. 4B). The phenotype observed in *mom-5* loss of function is therefore very similar to the phenotype observed in mutants for the Wnt ligands. All together, this suggests that MOM-5 is the main Wnt receptor involved in this process.

Interestingly, in a previous study it has been observed, using a rescuing MOM-5::GFP protein fusion (*zuIs145*), that at earlier developmental stages (during gastrulation) MOM-5 is transiently enriched at the posterior pole of several blastomeres during division (Park et al., 2004). We therefore tested whether MOM-5 could also be asymmetrically distributed at our later stage of interest (neurulation, epidermal enclosure) in the SMDD/AIY mother. Using the same MOM-5::GFP protein fusion (*zuIs145*) we observed a slight and transient enrichment of MOM-5 at the

posterior pole of the SMDD/AIY mother during mitosis (Fig. S6). In this line, MOM-5::GFP is expressed in every cell, therefore the asymmetry in the SMDD/AIY mother could be partially masked by signal from the neighboring cells. To circumvent this problem we expressed MOM-5::GFP in only a few neuronal progenitors using the *hlh-16* promoter as a driver (Bertrand et al., 2011). This promoter drives expression in the SMDD/AIY mother (red dot, Fig. 4C) and in a lateral cell (blue dot, Fig. 4C) but not in cells just anterior or posterior to the SMDD/AIY mother. Driving MOM-5::GFP expression using the *hlh-16* promoter does not perturb the generation of the AIY neurons (assessed with *ttx-3* expression at larval stage, n=100 animals analyzed). Using this transgenic line, we observed a clear and transient enrichment of MOM-5 at the posterior pole of the SMDD/AIY mother during mitosis (Fig. 4C) but not before or after mitosis. We then tested whether overriding the asymmetry of Wnt ligand expression by ubiquitous *hsp::cwn-2* overexpression would affect MOM-5 asymmetry. We indeed observed that *cwn-2* ubiquitous expression perturbs the localization of MOM-5 (Fig. 4C), suggesting that Wnt ligand asymmetry regulates MOM-5 asymmetry. Taken together, these data show that the Wnt receptor MOM-5 regulates the asymmetric division of the SMDD/AIY mother and is transiently enriched at its posterior pole in a Wnt regulated manner.

Transmembrane proteins of the Planar Cell Polarity signaling system (PCP) have been identified in *Drosophila* to regulate the local coordination of polarity between neighboring epithelial cells (Gray et al., 2011). PCP is divided in two pathways. The first pathway involves the transmembrane proteins Van Gogh, Flamingo and Frizzled. In this pathway, a Van Gogh / Flamingo complex on one cell interacts with a Frizzled / Flamingo complex on the neighboring cell. In the second pathway, the transmembrane protein Fat of one cell interacts with the transmembrane protein Dachsous of the neighboring cell. In *C. elegans*, there is one Van Gogh (VANG-1), one Flamingo (FMI-1), two Fat (CDH-3 and CDH-4) and one Dachsous (CDH-1) (Ackley, 2014). We analyzed the effect of loss-of-function mutations in each of them (*vang-1(tm1422)*, *fmi-1(rh308)*, *cdh-1(gk747)*, *cdh-3(pk87)*, *cdh-4(hd40)*). We did not observe any defect in the generation of the AIY neuron (Fig. S4). In addition, the SMDD/AIY mother is still elongated (Fig. S2A) and the orientation of this elongation is unaffected (Fig. S5A). There is also no major defect in the orientation of the division (Fig. S5B). As the two PCP pathways could act

redundantly, we analyzed the effect of a double mutant (*vang-1(tm1422); cdh-1(gk747)*) affecting both pathways. Again, we did not observe any major defect in the generation of the AIY neuron, the elongation of the SMDD/AIY mother or the orientation of the elongation and division (Fig. S2A, Fig. S4, Fig. S5). Taken together, these data suggest that PCP signaling does not play a key role in the terminal division of the SMDD/AIY mother.

The APC protein APR-1 regulates the asymmetric division of the SMDD/AIY neuronal progenitor and is enriched at the anterior pole.

The Wnt pathway regulates both the orientation of the SMDD/AIY mother cell and the asymmetry of daughter cell fates. To better understand how these two aspects are coordinated we first tried to determine which downstream cytoplasmic component could mediate both processes. APC is a good candidate as it is both a regulator of microtubules (cell shape), and a regulator of the transcriptional coactivator β-catenin (cell fate) (Williams and Fuchs, 2013). APC is a cytoplasmic protein that can be recruited to the cortex. *C. elegans* has one APC protein, APR-1 (Sawa and Korswagen, 2013). We tested whether APR-1 regulates the shape and division of the SMDD/AIY mother cell. We observed that, in a loss-of-function mutant of *apr-1* (*zh10*) or after *apr-1* RNAi knock down, the fate of the AIY neuron is affected (Fig. 5A). We detected both cases of loss and of duplication of AIY fate, which may reflect the dual role played by APR-1 in the Wnt/β-catenin asymmetry pathway: APR-1 can both promote the acquisition of anterior fate in the anterior daughter (for example in the larval T blast cell division (Mizumoto and Sawa, 2007)) or the acquisition of posterior fate in the posterior daughter (for example in the EMS endomesoderm precursor division of the early embryo (Nakamura et al., 2005; Rocheleau et al., 1997)). In the case of the SMDD/AIY mother cell, symmetrization of the division in *apr-1* loss of function may lead to loss of AIY fate or duplication of AIY fate depending on stochastic variability of protein levels between embryos.

After *apr-1* RNAi knock down the elongation of the SMDD/AIY mother is not affected (Fig. S2A) but the orientation of the cell is perturbed (Fig. 5B). In addition,

the orientation of the division is also affected (Fig. 5B). This suggests that APR-1 regulates the orientation of the SMDD/AIY mother and its asymmetric division.

Next, we wanted to determine if APR-1 is asymmetrically localized in the SMDD/AIY mother. We tagged the APR-1 protein with GFP using a fosmid reporter strategy and checked that the APR-1::GFP fusion obtained rescues an *apr-1* loss-of-function mutant (see material and methods). Using this construct, we observed that during interphase, when the SMDD/AIY mother cell is elongated, APR-1 is enriched at the anterior tip of the cell (Fig. 6A, B). This enrichment at the anterior cortex is still present when the cell is rounded during mitosis (Fig. 6B). After division, the APR-1 cortical signal remains stronger in the anterior daughter (SMDD) than in the posterior daughter (AIY) (Fig. 6B). We then tested whether ubiquitously expressing *cwn-2* (*hsp::cwn-2*) would affect APR-1 asymmetry. *cwn-2* ubiquitous expression perturbs the localization of APR-1 (Fig. 7A), suggesting that Wnt ligand asymmetry regulates APR-1 asymmetry. Finally, in a *mom-5(gk812)* loss-of-function mutant, we observed that APR-1 localization at the cortex is randomized (Fig. 7B), suggesting that the Wnt receptor MOM-5 regulates the anterior enrichment of APR-1. Taken together, these data are consistent with a model where during interphase APR-1 is enriched at the anterior cortex in a Wnt signaling dependent manner, leading to the orientation of the SMDD/AIY mother along the anteroposterior axis. Later, during division, APR-1 is still enriched at the anterior cortex, regulating the orientation of the division and the asymmetry of daughter cell fate.

DISCUSSION

A Model for the regulation of the terminal asymmetric division of embryonic neuronal progenitors in *C. elegans*.

In this article, we have analyzed the role of Wnt ligands in the regulation of terminal asymmetric divisions of embryonic neuronal progenitors in *C. elegans* embryos using the AIY neuron as a test lineage. Using time-controlled perturbations, we show that three Wnt ligands (CWN-1, CWN-2 and MOM-2) regulate the terminal division of the SMDD/AIY mother cell. We have also identified a role for the Wnt receptor MOM-5/Frizzled and the cortical protein APR-1/APC, which both present an asymmetric distribution in the SMDD/AIY mother during division. A simple explanation for our results is that Wnt ligands are directly read by the SMDD/AIY mother cell via the MOM-5 receptor and the downstream intracellular APR-1 protein (Fig. 8). However, as MOM-5 and APR-1 were removed globally it is also possible that loss in other cells contributes to the phenotype.

We have observed that the SMDD/AIY mother is elongated along the anteroposterior axis during interphase. The fact that the mother cell is elongated is independent of Wnt ligands, MOM-5 and APR-1, and could be a cell autonomous property. However, the orientation of this elongation depends on Wnt ligands, MOM-5 and APR-1. In wild type animals, this orientation correlates with the axis of Wnt differential expression (anteroposterior axis) and perturbations of the Wnt expression pattern affect the orientation suggesting that Wnt ligands play an instructive role in the orientation of the mother cell. During interphase, APR-1 is enriched at the anterior cortex of the mother cell in a Wnt regulated manner and affects the orientation of the elongation. However, how APR-1 regulates the orientation of the elongation remains to be determined. In other contexts, it has been observed that APR-1, similar to its vertebrate ortholog APC, is able to interact with the cytoskeleton. For example, APR-1 can bind and stabilize microtubules plus ends (Sugioka et al., 2018; Sugioka et al., 2011; Sugioka and Sawa, 2012). In addition, APR-1 can control actin reorganization via the Rac pathway (Cabello et al., 2010; Gomez-Orte et al., 2013). Therefore, Wnt ligands, by inducing an accumulation of APR-1 at the anterior

cortex, could affect the organization of the cytoskeleton, orienting the elongation of the cell along the anteroposterior axis of the embryo.

During mitosis, the SMDD/AIY mother becomes rounded and divides along the anteroposterior axis. The orientation of the division is also regulated by Wnt ligands (CWN-1, CWN-2 and MOM-2), MOM-5/Frizzled and APR-1/APC. Interestingly, both in cultures and embryos, cells tend to divide along their long axis, a phenomenon named Hertwig's rule (Cadart et al., 2014), although the mechanism that helps cells remember the orientation of their interphase long axis during rounding remains poorly characterized. As both the elongation and division of the SMDD/AIY mother cell are oriented along the anteroposterior axis, it is possible that the long axis of the SMDD/AIY mother cell during interphase determines the orientation of the division following Hertwig's rule. In addition, during division, APR-1 is enriched at the anterior pole of the mother cell. As APR-1 can interact with astral microtubules (Sugioka et al., 2018; Sugioka et al., 2011; Sugioka and Sawa, 2012) it could also directly affect the orientation of the mitotic spindle. During division we also detected a slight enrichment of MOM-5 at the posterior pole. However, the role of this weak and transient enrichment is unclear.

After division, the anterior and posterior daughters acquire different neuronal fates, the expression of the key transcription factor TTX-3 disappearing from the anterior neuron (SMDD) while being maintained in the posterior neuron (AIY) (Bertrand and Hobert, 2009). Here we show that this asymmetry of cell fate is regulated by the Wnt ligands CWN-1, CWN-2 and MOM-2. In addition, our timing experiments indicate that the Wnt ligands act on the mother cell at the time of cell division to affect the daughter cell fates rather than directly on the daughters themselves long after division. This is likely achieved by the regulation of the localization or activity of Wnt pathway cortical components during the division as suggested for the asymmetric division of the endomesoderm precursor EMS in the embryo or the epidermal T blast cell in the larva (reviewed in Bertrand, 2016; Sawa and Korswagen, 2013). In the case of the SMDD/AIY mother cell, we have observed that APR-1 is enriched at the anterior cortex during the division, is asymmetrically inherited, and regulates the asymmetry of cell fate. How does APR-1 asymmetry generate different daughter cell fates? We have previously shown that the difference

of fate between the SMDD and AIY neurons is due to different concentrations of the transcriptional regulators SYS-1/β-catenin and POP-1/TCF in the daughter nuclei just after cell division (Bertrand and Hobert, 2009). In the posterior daughter nucleus, SYS-1 concentration is high, POP-1 concentration is low and POP-1 bound to SYS-1 activates transcription. In the anterior daughter nucleus, SYS-1 concentration is low, POP-1 concentration is high and POP-1 free of SYS-1 represses transcription (Bertrand and Hobert, 2009). Interestingly, in the EMS cell of the early embryo, it has been observed that, during mitosis, APR-1 accumulation at the anterior cortex leads to an asymmetry in astral microtubules that generates a lower nuclear export of POP-1 from the anterior nucleus than posterior nucleus (Sugioka et al., 2011). In addition, in the EMS cell and larval epidermal blast cell divisions, APR-1 generates an asymmetry in SYS-1 levels between daughter cells by regulating SYS-1 degradation (Baldwin and Phillips, 2014; Huang et al., 2007). In the case of the SMDD/AIY mother, it seems therefore likely that APR-1 asymmetry regulates POP-1 and SYS-1 nuclear asymmetries, which result in the acquisition of different fates in the daughter neurons SMDD and AIY. In addition to regulating the localization of APR-1, the Wnt ligands and their MOM-5 receptor could also regulate APR-1 activity for example by modulating APR-1 interaction with other components of the destruction complex that regulates SYS-1 degradation.

The Wnt pathway regulates both the orientation of the division and the asymmetry of daughter cell fates. However, defects in daughter cell fate asymmetry is unlikely to be a simple direct consequence of defects in orientation, as for example Wnt ligand loss- or gain-of-functions lead to the same orientation defects but different defects in terms of fates (loss of AIY fate versus duplication of AIY fate). This can be explained by the fact that the Wnt ligands, the MOM-5 receptor and APR-1 not only regulate the orientation of the division but also directly regulate during the division the generation of POP-1 and SYS-1 asymmetries and therefore daughter cell fates.

Wnt ligands have been previously implicated in the orientation of blastomere divisions in earlier embryos (during gastrulation) (Bischoff and Schnabel, 2006; Zacharias et al., 2015), however how Wnt ligands regulate these divisions remains unclear. In addition, MOM-5 and APR-1 have been observed to be asymmetrically localized in the early embryo (Park et al., 2004; Sugioka et al., 2018; Sugioka et al.,

2011). Our results extend these observations to later stages of embryogenesis (terminal divisions of neuronal precursors during epidermal enclosure), suggesting that they may be general features during embryonic development.

We noticed that the phenotypes of loss- or gain-of-function of Wnt ligands are only partially penetrant both in terms of orientation and fate. This could be explained by the fact that, in our experimental settings, the loss- or gain-of-function is only partial. For example, the *mom-2* thermosensitive allele that we used is only a partial loss-of-function. In addition, the ubiquitous overexpression may not be high enough to completely erase the endogenous asymmetry of Wnt expression. Another possibility is that another cue acts in parallel to Wnt in the polarization along the anteroposterior axis, such as other chemical or mechanical cues. Finally, it is also possible that part of the cell polarity is inherited from earlier stages in an autonomous manner.

Regulation of tissue polarization by Wnt ligands

Wnt ligands have been proposed to play an instructive role in the polarization of asymmetric cell divisions in several systems such as the early endomesoderm precursor cell EMS and the larval T blast cell of *C. elegans* (Goldstein et al., 2006) or mammalian ES cells (Habib et al., 2013). In addition, gradients of Wnt ligands have been suggested to polarize fields of cells such as the vulval precursors cells of *C. elegans* (Green et al., 2008), the wing of *Drosophila* (Wu et al., 2013) or the vertebrate limb bud (Gros et al., 2010). However, the molecular mechanism by which Wnt ligands can polarize fields of cells remains poorly characterized.

Wnt can act as a short- or long-range signal depending on tissue context. Wnt proteins are lipid modified but can travel away from their source using carriers such as lipoprotein particles or extracellular vesicles (Langton et al., 2016). For example, in the *C. elegans* larva, it has been observed that the Wnt EGL-20 spreads from its source in the extracellular space to form a long-range gradient (Coudreuse et al., 2006; Pani and Goldstein, 2018). Therefore, each cell of the tissue may be subjected to slightly different Wnt concentration at their two poles. Each cell may be able to

sense this small difference, which could then be amplified by an intracellular mechanism involving the receptor and leading to a robust cell polarity (Tan et al., 2013). While this simple mechanism is attractive, it still needs further testing and the amplification mechanism has to be clarified. It will be especially important in the future to analyze in detail the dynamics of Wnt ligands, their receptors and downstream transducers during the polarization process *in vivo* using quantitative live imaging. The *C. elegans* embryo and its neuronal progenitors, with its fast development and transparency, is an interesting system for such future studies.

MATERIALS AND METHODS

Expression constructs and transgenic strains

All experiments were performed on *C. elegans* hermaphrodites.

For Wnt overexpression experiments, the *hsp::cwn-2* extrachromosomal array *kyEx1369* (Kennerdell et al., 2009) was integrated using UV irradiation to generate the *vbaIs5* line and backcrossed four times before analysis.

For MOM-5 localization in the SMDD/AIY mother cell, a construct where a GFP C-terminal tagged version of MOM-5 is expressed under the control of the *hlh-16* promoter -514 was generated by cloning the *mom-*5 cDNA between the XbaI and XmaI sites of the hlh-16prom(-514)::gfp vector (Bertrand et al., 2011). The construct was injected at 50 ng/μl with a pRF4 coinjection marker to generate the extrachromosomal array *vbaEx119*.

The plasmid to produce *mom-5* dsRNAs was generated by cloning the full *mom-5* cDNA between the XbaI and MluI sites of the RNAi vector pDD129.36. The plasmid was then transformed into HT115 bacteria to produce dsRNAs.

For APR-1 localization, a fosmid where the APR-1 protein is tagged in frame with GFP was obtained from the TransgeneOme project (M. Sarov) (Sarov et al., 2012). It was injected at 100 ng/μl with the pRF4 coinjection marker to generate the extrachromosomal array *vbaEx56*. The array was subsequently integrated using X-ray irradiation to generate the *vbaIs34* line and backcrossed three times before analysis. The *vbaIs34* transgene rescues the zygotic lethality induced by the *apr-1(zh10)* loss of function mutant showing that the fusion protein is functional.

The MOM-2::YFP, CWN-1::YFP and CWN-2::YFP protein fusions were generated by C-terminal insertion of the YFP sequence with a SGGGGS linker in the respective fosmids (WRM0637bH02, WRM0614bH03, WRM0622cB04) by fosmid

recombineering (Tursun et al., 2009). They were injected at 150 ng/μl with the pRF4 coinjection marker and subsequently integrated using X-ray irradiation to generate the *vbaIs40*, *vbaIs38* and *vbaIs43* lines respectively, and backcrossed three times before analysis.

Temperature shifts

For strains containing the *mom-2(ne874ts)* thermosensitive allele, embryos were mounted at the two-cell stage on a 5% agar pad between a slide and a coverslip, incubated at 15°C (permissive temperature) until the desired upshift time, and then incubated at 25°C (restrictive temperature) until analysis. The upshift time was determined based on previous experiments showing that in the early embryo defects were observed 30 min after the shift to restrictive temperature (Nakamura et al., 2005).

For strains containing the *hsp::cwn-2 (vbaIs5)* transgene, embryos were mounted at the two-cell stage on a 5% agar pad between a slide and a coverslip, incubated at 20°C until the desired heat shock time, then incubated at 37°C for 20 minutes, and subsequently put back at 20°C until analysis.

Local heat shock using a laser

The infrared laser used is a Keopsys 1480 nm continuous wave Raman fiber laser. It is set on a Nikon TE Eclipse microscope with a spinning disk unit (Yokogawa CSU-X) and coupled to an Andor iXon3 DU897 camera. We calibrated the local temperature increase in embryos using a red dye (rhodamine) fed to mothers. Upon increase of temperature the fluorescence intensity of rhodamine decreases. We also checked the ability of the system to induce local expression using a *hsp::gfp* transgene.

For the experiments, two-cell stage embryos were mounted on a 5% agar pad between a slide and a coverslip, grown at 20° for 90 minutes and then locally heat shocked (laser power 3250 mA for 45 seconds). The local heat shock was performed

laterally or posteriorly (as a negative control). Embryos were then incubated at 20° before analysis.

RNAi treatments

RNAi was performed on a strain containing the *ttx-3p::gfp* transgene and the *rrf-3(pk1426)* sensitizing mutation (Simmer et al., 2003). Hermaphrodites were grown from L4 stage at 20° on bacteria containing a plasmid expressing dsRNAs (plasmid generated here for *mom-5*; mv-K04G2.8b clone from Vidal library for *apr-1*; empty L4440 vector for negative control). Embryos produced by these hermaphrodites were then mounted at the two-cell stage on a 5% agar pad between a slide and a coverslip, and incubated at 20°C until analysis at epidermal enclosure stage or hatching.

Imaging

Standard observations were performed with a Zeiss Axioplan 2 epifluorescence microscope, a Zeiss AxioCam MRm camera and the AxioVision software.

Time lapse imaging was performed using a spinning disc confocal microscope (Nikon Eclipse Ti microscope, spinning disc module Yokogawa CSU-X1, EMCCD camera Photometrics Evolve, Metamorph software). Embryos were mounted at the two-cell stage on a 5% agar pad between a slide and a coverslip, and incubated at 20°C until the right stage for recording was reached.

Measure of elongation, orientation, MOM-5, APR-1 and Wnt levels

At our stage of interest (epidermal enclosure) the two SMDD/AIY mothers are located on the ventral surface of the embryo. At this stage, when mounted between a slide and a coverslip the embryo displays either a ventral view or a dorsal view. Only ventral views were analyzed. After fluorescent z-stack acquisition, the plane where the SMDD/AIY mother presents the maximal surface was selected (plane going

through the center of the cell; the SMDD/AIY mother usually appears on 3 successive planes, distance between planes 1 μm). The contour of the cell is then drawn manually and the elongation factor and angle of orientation are then determined using the fit ellipse function on ImageJ. The elongation factor corresponds to the ratio between the lengths of the major axis and minor axis of the fit ellipse. The angle of orientation corresponds to the angle between the major axis of the fit ellipse and the anteroposterior axis of the embryo.

For MOM-5::GFP levels quantification in the *hlh-16p::mom-5::gfp (vbaEx119)* line, the mean fluorescence intensity was measured at the posterior and anterior membrane using ImageJ. The mean cytoplasmic signal was then subtracted from these values to get the membrane enrichment at the posterior and anterior. The ratio of posterior versus anterior enrichment was then calculated.

For MOM-5::GFP and APR-1::GFP levels quantification in the *zuIs145* and *vbaIs34* lines, the fluorescence intensity profile along the cell membrane was measured using ImageJ. The mean cytoplasmic signal was then subtracted from these values to get the membrane enrichment profile.

For CWN-1::YFP and CWN-2::YFP levels quantifications using ImageJ an average intensity projection of the planes containing the SMDD/AIY mothers (identified with *ttx-3p::mCherry*, *otIs181*) was performed, a box containing the two SMDD/AIY mothers was subsequently defined and the intensity profile was then plotted along the anteroposterior axis. Background signal was then subtracted.

Statistics

For comparisons of proportions between wild type and mutant animals, a non-parametric Fisher's exact test (two-tailed) was performed. For comparison of angles between wild type and mutant animals, angles were first binned in two groups: biased towards the anteroposterior axis (-45° to 0° and 0° to +45°) and biased towards the mediolateral axis (-90° to -45° and +45° to +90°). A non-parametric

679 Fisher's exact test (two-tailed) was then performed. For comparisons of MOM-5
680 levels a non-parametric Mann-Whitney test (two-tailed) was performed.
681

ACKNOWLEDGMENTS

We thank C. Couillault for expert assistance with injections and molecular biology; H. Sawa, C. Bargmann, Y. Kohara and M. Sarov for strains and reagents; members of our labs for comments on the manuscript. Imaging was performed on PiCSL-FBI core facility (IBDM, AMU-Marseille) supported by the French National Research Agency through the “Investments for the Future" program (France-BioImaging, ANR-10-INBS-04). Some strains were provided by the CGC, which is funded by NIH Office of Research Infrastructure Programs (P40 OD010440).

COMPETING INTERESTS

The authors declare no competing or financial interests.

FUNDING

This work was funded by an ATIP/Avenir startup grant from CNRS/INSERM to V.B. and grants from the Agence Nationale de la Recherche (ANR-14-CE11-0001 and ANR-11-LABX-0054) to V.B. and P.-F.L.

FIGURE LEGENDS

Fig. 1. The SMDD/AIY mother cell is elongated and divides along the anteroposterior axis.

(A) Scheme of the ventral side of a *C. elegans* embryo at epidermal enclosure (neurulation). Each green dot represents the nucleus of a neuronal progenitor.

(B) Terminal division of the SMDD/AIY mother cell.

(C) Three images extracted from a time lapse movie following the SMDD/AIY mother cell labeled with GFP (*ttx-3p::gfp*, *mgIs18*). Embryo at epidermal enclosure stage, ventral view, scale bar = 5 μm.

(D) Elongation factor of the SMDD/AIY mother. Mean value of 10 cells followed by time-lapse microscopy every 2 minutes (error bars = s.d.). Time 0 corresponds to the point when the cell enters division. Elongation is not measured at time 2 because the SMDD/AIY mother no longer exists.

(E) Deviation of the main axis of the SMDD/AIY mother from the anteroposterior axis. Mean of the absolute angle values (0-90 degrees), same conditions as (D). Due to rounding during mitosis, the angle is not measured at t = 0. At t = 2, the value represents the deviation of the axis made by the centers of the two daughters from the anteroposterior axis (error bars = s.d.).

Fig. 2. Effect of Wnt mutants and overexpression on AIY fate.

(A) Expression of *Wnt* ligands in the embryo at epidermal enclosure stage. Transcriptional reporters with the *cis*-regulatory regions of the *Wnt* genes driving the expression of a nuclear gfp (*cwn-1p::gfp*, *deEx101* ; *cwn-2p::gfp*, *deEx103* ; *mom-2p::gfp*, *deEx104*, *lin-44p::gfp deEx100*, *egl-20p::gfp deEx102*). Ventral view, red dots = location of the SMDD/AIY mothers, scale bar = 10 μm.

(B) Percentage of animals with a loss of AIY fate (marked with *ttx-3p::gfp*) in Wnt mutants. Left graph: as *cwn-1(ok546)* and *cwn-2(ok895)* are viable, analysis was performed at L4 larval stage (n = 100 animals for each genotype). Right graph: as *mom-2* mutants are lethal, a temperature sensitive allele was used (*ne874ts*); embryos were shifted to the restrictive temperature at 240 minutes in Sulston timetable and analyzed at hatching (n = 97, 23, 30, 24, 30 animals respectively for each genotype). Error bars = s.e.p., *** p = 0.0001 Fisher.

(C) Percentage of animals with duplication of AIY fate in *cwn-2* ubiquitous overexpression. Expression of the *hsp::cwn-2 (vbaIs5)* transgene was induced at various time points by heat shock and animals were then analyzed at hatching (*hsp::cwn-2*: n = 114, 102, 97, 74, 62, 57 animals respectively for each time point; wild type: n = 71, 60, 42, 40, 28, 32 animals respectively for each time point). Time in minutes relative to the first division (Sulston timetable), the SMDD/AIY mother divides at 300 minutes. Error bars = s.e.p., *** p = 0.0003, ** p = 0.006 Fisher.
(D) Expression of *ttx-3* (*ttx-3p::gfp*) at hatching. At that time expression is restricted to AIY in wild type animals and excluded from its sister neuron SMDD. In *mom-2(ne874ts)*; *cwn-1(ok546)*; *cwn-2(ok895)* triple mutants expression of *ttx-3* is lost in AIY. In *hsp::cwn-2* overexpressing animals, *ttx-3* is ectopically expressed in the sister neuron SMDD. Anterior is left, scale bar = 5 μm.

Fig. 3. Effect of Wnt mutants and overexpression on orientation.
(A) SMDD/AIY mother cell before division (left), or SMDD and AIY neurons just after division (right) marked with *ttx-3p::gfp*. In *mom-2*; *cwn-1*; *cwn-2* triple mutants or *hsp::cwn-2* overexpressing animals the orientation of the SMDD/AIY mother cell and of its division are perturbed. Scale bar = 5 μm.
(B) Orientation of the elongation of the SMDD/AIY mother cell before division in Wnt mutant embryos, *** p = 0.001 Fisher. Embryos containing the *mom-2(ne874ts)* allele were shifted to the restrictive temperature at 240 minutes in Sulston timetable. Rose plot: 0° anterior, -90° lateral, +90° medial, circular grid 10%, n = number of cells.
(C) Orientation of the division of the SMDD/AIY mother cell in Wnt mutant embryos, *** p = 0.002 Fisher.
(D) Orientation of the elongation of the SMDD/AIY mother cell before division in wild type or *hsp::cwn2* heat shocked embryos, ** p = 0.007 Fisher. Expression of the *hsp::cwn-2* transgene was induced at 240 minutes in Sulston timetable by heat shock.
(E) Orientation of the division of the SMDD/AIY mother cell in wild type or *hsp::cwn2* heat shocked embryos, ** p = 0.01 Fisher.

Fig. 4. Effect and localization of MOM-5.

(A) Percentage of animals with a loss or duplication of AIY fate (marked with *ttx-3p::gfp* at hatching) in *mom-5* mutants or RNAi. Error bars = s.e.p.; *** p = $2x10^{-15}$ for mutants, *** p = $1x10^{-6}$ for RNAi, ns: not significant, Fisher; n = number of animals.
(B) Orientation of the elongation of the SMDD/AIY mother cell before division or of the division of the SMDD/AIY mother cell in *control(RNAi)* or *mom-5(RNAi)* embryos. Same plot as Fig. 3, * p = 0.049 for elongation, * p = 0.016 for division, Fisher.
(C) Localization of MOM-5::GFP proteins in the SMDD/AIY mother cell during mitosis (*hlh-16p::mom-5::gfp*, *vbaEx119*). The *hlh-16* promoter drives expression of MOM-5::GFP in the SMDD/AIY mother (red dot) and a cell lateral to the SMDD/AIY mother (blue dot, the mother of the SIAD and SIBV neurons) but not in the cells just anterior or posterior to the SMDD/AIY mother, allowing quantification of MOM-5 levels at the anterior and posterior poles of the SMDD/AIY mother. Pictures: SMDD/AIY mother cell just before cytokinesis in wild type or *hsp::cwn-2* overexpressing animals, ventral view, scale bar = 5 μm. Graph: ratio of MOM-5::GFP fluorescence levels between the posterior pole and the anterior pole of the SMDD/AIY mother cell just before cytokinesis in wild type non heat shocked, wild type heat shocked or *hsp::cwn2* heat shocked embryos (heat shock at 240 minutes in Sulston timetable). The black box represents the median and quartiles; the whiskers represent the 9th and 91st percentiles; n = number of cells, ns: not significant, *** p = 0.0015 Mann-Whitney.

Fig. 5. Effect of APR-1.

(A) Percentage of animals with a loss or duplication of AIY fate (marked with *ttx-3p::gfp* at hatching) in *apr-1* mutants or RNAi. Error bars = s.e.p.; for mutants: *** p = $8x10^{-7}$ and ** p = 0.006; for RNAi: *** p = $2x10^{-6}$ and * p = 0.02; Fisher; n = number of animals.
(B) Orientation of the elongation of the SMDD/AIY mother cell before division or of the division of the SMDD/AIY mother cell in *control(RNAi)* or *apr-1(RNAi)* embryos. Same plot as Fig.3, n = number of cells. * p = 0.014 for elongation, *** p = 0.003 for division, Fisher.

Fig. 6. Localization of APR-1.

(A) Localization of APR-1::GFP (*vbaIs34*, in white) in the SMDD/AIY mother cell during interphase. The perimeter of the SMDD/AIY mother cell (identified with *ttx-3p::mCherry*, *otIs181*) is indicated in yellow. Ventral view, scale bar = 5 μm.
(B) APR-1::GFP fluorescence intensity profile at the cortex of the cell. The x-axis presents the position at the circumference of the cell with the anterior pole in the middle and posterior pole at both ends. The grey curves represent individual cells and the red curve represents the mean curve. Top left: measure in the SMDD/AIY mother during interphase (n= 11 cells analyzed). Top right and bottom: the same cells were analyzed during mitosis and after cytokinesis; the signal in the mother and the two daughter cells was normalized to the mean signal of the mother (n= 10 divisions).

Fig. 7. Effect of Wnt ubiquitous expression or *mom-5* loss of function on APR-1 localization.
(A) APR-1::GFP (*vbaIs34*) in the SMDD/AIY mother in wild type heat shocked or *hsp::cwn-2* heat shocked animals (heat shock at 240 minutes in Sulston timetable). Pictures: the perimeter of the SMDD/AIY mother cell is indicated in yellow. Ventral view, scale bar = 3 μm. Graph: fluorescence intensity profile at the cortex, the x-axis presents the position at the circumference of the cell with the anterior pole in the middle and posterior pole at both ends. The grey curves represent individual cells and the red curve represents the mean curve, n= 11 cells for wild type and 15 cells for mutants.
(B) Same as panel A in wild type or *mom-5(gk812)* mutant background, n= 16 cells for wild type and 10 cells for mutants.

Fig. 8. A model for the regulation of neuronal progenitor terminal asymmetric divisions.

REFERENCES

Ackley, B. D. (2014). Wnt-signaling and planar cell polarity genes regulate axon guidance along the anteroposterior axis in C. elegans. *Dev Neurobiol* **74**, 781-796.

Baldwin, A. T. and Phillips, B. T. (2014). The tumor suppressor APC differentially regulates multiple beta-catenins through the function of axin and CKIalpha during C. elegans asymmetric stem cell divisions. *J Cell Sci* **127**, 2771-2781.

Bertrand, V. (2016). beta-catenin-driven binary cell fate decisions in animal development. *Wiley Interdiscip Rev Dev Biol* **5**, 377-388.

Bertrand, V., Bisso, P., Poole, R. J. and Hobert, O. (2011). Notch-dependent induction of left/right asymmetry in C. elegans interneurons and motoneurons. *Curr Biol* **21**, 1225-1231.

Bertrand, V. and Hobert, O. (2009). Linking asymmetric cell division to the terminal differentiation program of postmitotic neurons in C. elegans. *Dev Cell* **16**, 563-575.

Bielen, H. and Houart, C. (2014). The Wnt cries many: Wnt regulation of neurogenesis through tissue patterning, proliferation, and asymmetric cell division. *Dev Neurobiol* **74**, 772-780.

Bischoff, M. and Schnabel, R. (2006). A posterior centre establishes and maintains polarity of the Caenorhabditis elegans embryo by a Wnt-dependent relay mechanism. *PLoS Biol* **4**, e396.

Cabello, J., Neukomm, L. J., Gunesdogan, U., Burkart, K., Charette, S. J., Lochnit, G., Hengartner, M. O. and Schnabel, R. (2010). The Wnt pathway controls cell death engulfment, spindle orientation, and migration through CED-10/Rac. *PLoS Biol* **8**, e1000297.

Cadart, C., Zlotek-Zlotkiewicz, E., Le Berre, M., Piel, M. and Matthews, H. K. (2014). Exploring the function of cell shape and size during mitosis. *Dev Cell* **29**, 159-169.

Coudreuse, D. Y., Roel, G., Betist, M. C., Destree, O. and Korswagen, H. C. (2006). Wnt gradient formation requires retromer function in Wnt-producing cells. *Science* **312**, 921-924.

Delaunay, D., Cortay, V., Patti, D., Knoblauch, K. and Dehay, C. (2014). Mitotic spindle asymmetry: a Wnt/PCP-regulated mechanism generating asymmetrical division in cortical precursors. *Cell Rep* **6**, 400-414.

Gleason, J. E., Szyleyko, E. A. and Eisenmann, D. M. (2006). Multiple redundant Wnt signaling components function in two processes during C. elegans vulval development. *Dev Biol* **298**, 442-457.

Goldstein, B., Takeshita, H., Mizumoto, K. and Sawa, H. (2006). Wnt signals can function as positional cues in establishing cell polarity. *Dev Cell* **10**, 391-396.

Gomez-Orte, E., Saenz-Narciso, B., Moreno, S. and Cabello, J. (2013). Multiple functions of the noncanonical Wnt pathway. *Trends Genet* **29**, 545-553.

Gotz, M. and Huttner, W. B. (2005). The cell biology of neurogenesis. *Nat Rev Mol Cell Biol* **6**, 777-788.

Gray, R. S., Roszko, I. and Solnica-Krezel, L. (2011). Planar cell polarity: coordinating morphogenetic cell behaviors with embryonic polarity. *Dev Cell* **21**, 120-133.

Green, J. L., Inoue, T. and Sternberg, P. W. (2008). Opposing Wnt pathways orient cell polarity during organogenesis. *Cell* **134**, 646-656.

Gros, J., Hu, J. K., Vinegoni, C., Feruglio, P. F., Weissleder, R. and Tabin, C. J. (2010). WNT5A/JNK and FGF/MAPK pathways regulate the cellular events shaping the vertebrate limb bud. *Curr Biol* **20**, 1993-2002.

Habib, S. J., Chen, B. C., Tsai, F. C., Anastassiadis, K., Meyer, T., Betzig, E. and Nusse, R. (2013). A localized Wnt signal orients asymmetric stem cell division in vitro. *Science* **339**, 1445-1448.

Hartenstein, V. and Stollewerk, A. (2015). The evolution of early neurogenesis. *Dev Cell* **32**, 390-407.

Harterink, M., Kim, D. H., Middelkoop, T. C., Doan, T. D., van Oudenaarden, A. and Korswagen, H. C. (2011). Neuroblast migration along the anteroposterior axis of C. elegans is controlled by opposing gradients of Wnts and a secreted Frizzled-related protein. *Development* **138**, 2915-2924.

Huang, S., Shetty, P., Robertson, S. M. and Lin, R. (2007). Binary cell fate specification during C. elegans embryogenesis driven by reiterated reciprocal asymmetry of TCF POP-1 and its coactivator beta-catenin SYS-1. *Development* **134**, 2685-2695.

Kaletta, T., Schnabel, H. and Schnabel, R. (1997). Binary specification of the embryonic lineage in Caenorhabditis elegans. *Nature* **390**, 294-298.

Kamei, Y., Suzuki, M., Watanabe, K., Fujimori, K., Kawasaki, T., Deguchi, T., Yoneda, Y., Todo, T., Takagi, S., Funatsu, T., et al. (2009). Infrared laser-mediated gene induction in targeted single cells in vivo. *Nat Methods* **6**, 79-81.

Kennerdell, J. R., Fetter, R. D. and Bargmann, C. I. (2009). Wnt-Ror signaling to SIA and SIB neurons directs anterior axon guidance and nerve ring placement in C. elegans. *Development* **136**, 3801-3810.

Langton, P. F., Kakugawa, S. and Vincent, J. P. (2016). Making, Exporting, and Modulating Wnts. *Trends Cell Biol* **26**, 756-765.

Mizumoto, K. and Sawa, H. (2007). Cortical beta-catenin and APC regulate asymmetric nuclear beta-catenin localization during asymmetric cell division in C. elegans. *Dev Cell* **12**, 287-299.

Murgan, S., Kari, W., Rothbacher, U., Iche-Torres, M., Melenec, P., Hobert, O. and Bertrand, V. (2015). Atypical Transcriptional Activation by TCF via a Zic Transcription Factor in C. elegans Neuronal Precursors. *Dev Cell* **33**, 737-745.

Nakamura, K., Kim, S., Ishidate, T., Bei, Y., Pang, K., Shirayama, M., Trzepacz, C., Brownell, D. R. and Mello, C. C. (2005). Wnt signaling drives WRM-1/beta-catenin asymmetries in early C. elegans embryos. *Genes Dev* **19**, 1749-1754.

Nusse, R. and Clevers, H. (2017). Wnt/beta-Catenin Signaling, Disease, and Emerging Therapeutic Modalities. *Cell* **169**, 985-999.

Pani, A. M. and Goldstein, B. (2018). Direct visualization of a native Wnt in vivo reveals that a long-range Wnt gradient forms by extracellular dispersal. *Elife* **7**.

Park, F. D., Tenlen, J. R. and Priess, J. R. (2004). C. elegans MOM-5/frizzled functions in MOM-2/Wnt-independent cell polarity and is localized asymmetrically prior to cell division. *Curr Biol* **14**, 2252-2258.

Phillips, B. T. and Kimble, J. (2009). A new look at TCF and beta-catenin through the lens of a divergent C. elegans Wnt pathway. *Dev Cell* **17**, 27-34.

Rocheleau, C. E., Downs, W. D., Lin, R., Wittmann, C., Bei, Y., Cha, Y. H., Ali, M., Priess, J. R. and Mello, C. C. (1997). Wnt signaling and an APC-related gene specify endoderm in early C. elegans embryos. *Cell* **90**, 707-716.

Sarov, M., Murray, J. I., Schanze, K., Pozniakovski, A., Niu, W., Angermann, K., Hasse, S., Rupprecht, M., Vinis, E., Tinney, M., et al. (2012). A genome-scale resource for in vivo tag-based protein function exploration in C. elegans. *Cell* **150**, 855-866.

Sawa, H. and Korswagen, H. C. (2013). Wnt signaling in C. elegans. *WormBook*, 1-30.

Simmer, F., Moorman, C., van der Linden, A. M., Kuijk, E., van den Berghe, P. V., Kamath, R. S., Fraser, A. G., Ahringer, J. and Plasterk, R. H. (2003).

Genome-wide RNAi of C. elegans using the hypersensitive rrf-3 strain reveals novel gene functions. *PLoS Biol* **1**, E12.

Sugioka, K., Fielmich, L. E., Mizumoto, K., Bowerman, B., van den Heuvel, S., Kimura, A. and Sawa, H. (2018). Tumor suppressor APC is an attenuator of spindle-pulling forces during C. elegans asymmetric cell division. *Proc Natl Acad Sci U S A* **115**, E954-E963.

Sugioka, K., Mizumoto, K. and Sawa, H. (2011). Wnt regulates spindle asymmetry to generate asymmetric nuclear beta-catenin in C. elegans. *Cell* **146**, 942-954.

Sugioka, K. and Sawa, H. (2012). Formation and functions of asymmetric microtubule organization in polarized cells. *Curr Opin Cell Biol* **24**, 517-525.

Sulston, J. E., Schierenberg, E., White, J. G. and Thomson, J. N. (1983). The embryonic cell lineage of the nematode Caenorhabditis elegans. *Dev Biol* **100**, 64-119.

Tan, R. Z., Ji, N., Mentink, R. A., Korswagen, H. C. and van Oudenaarden, A. (2013). Deconvolving the roles of Wnt ligands and receptors in sensing and amplification. *Mol Syst Biol* **9**, 631.

Tursun, B., Cochella, L., Carrera, I. and Hobert, O. (2009). A toolkit and robust pipeline for the generation of fosmid-based reporter genes in C. elegans. *PLoS One* **4**, e4625.

Wenick, A. S. and Hobert, O. (2004). Genomic cis-regulatory architecture and trans-acting regulators of a single interneuron-specific gene battery in C. elegans. *Dev Cell* **6**, 757-770.

Williams, S. E. and Fuchs, E. (2013). Oriented divisions, fate decisions. *Curr Opin Cell Biol* **25**, 749-758.

Woodhead, G. J., Mutch, C. A., Olson, E. C. and Chenn, A. (2006). Cell-autonomous beta-catenin signaling regulates cortical precursor proliferation. *J Neurosci* **26**, 12620-12630.

Wu, J., Roman, A. C., Carvajal-Gonzalez, J. M. and Mlodzik, M. (2013). Wg and Wnt4 provide long-range directional input to planar cell polarity orientation in Drosophila. *Nat Cell Biol* **15**, 1045-1055.

Zacharias, A. L., Walton, T., Preston, E. and Murray, J. I. (2015). Quantitative Differences in Nuclear beta-catenin and TCF Pattern Embryonic Cells in C. elegans. *PLoS genetics* **11**, e1005585.

Zhang, J., Woodhead, G. J., Swaminathan, S. K., Noles, S. R., McQuinn, E. R., Pisarek, A. J., Stocker, A. M., Mutch, C. A., Funatsu, N. and Chenn, A.

(2010). Cortical neural precursors inhibit their own differentiation via N-cadherin maintenance of beta-catenin signaling. *Dev Cell* **18**, 472-479.

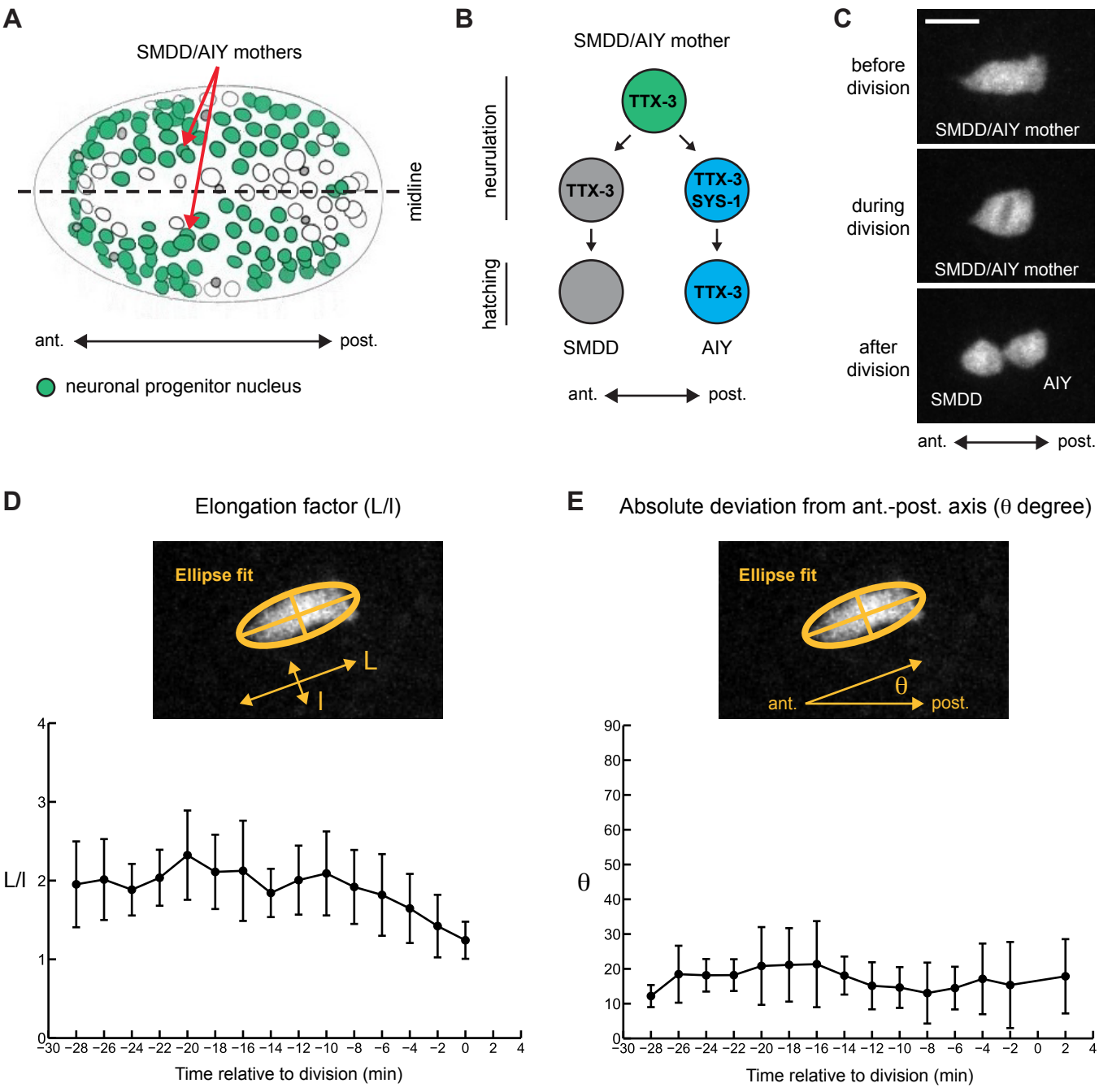
A
SMDD/AIY mothers
midline
ant.
post.
neuronal progenitor nucleus
B
SMDD/AIY mother
neurulation
hatching
TTX-3
TTX-3
TTX-3 SYS-1
TTX-3
SMDD
AIY
ant.
post.
C
before division
SMDD/AIY mother
during division
SMDD/AIY mother
after division
SMDD
AIY
ant.
post.
D
Elongation factor (L/I)
Ellipse fit
L
I
L/I
Time relative to division (min)
E
Absolute deviation from ant.-post. axis (θ degree)
Ellipse fit
ant.
θ
post.
θ
Time relative to division (min)

Figure 1

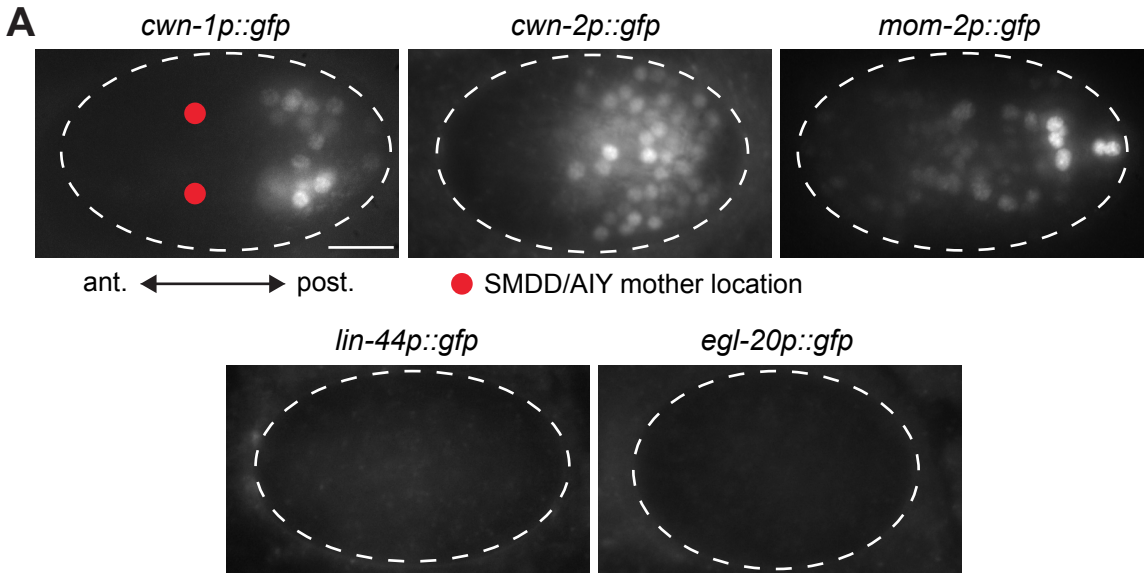
A
cwn-1p::gfp
cwn-2p::gfp
mom-2p::gfp
ant.
post.
SMDD/AIY mother location
lin-44p::gfp
egl-20p::gfp

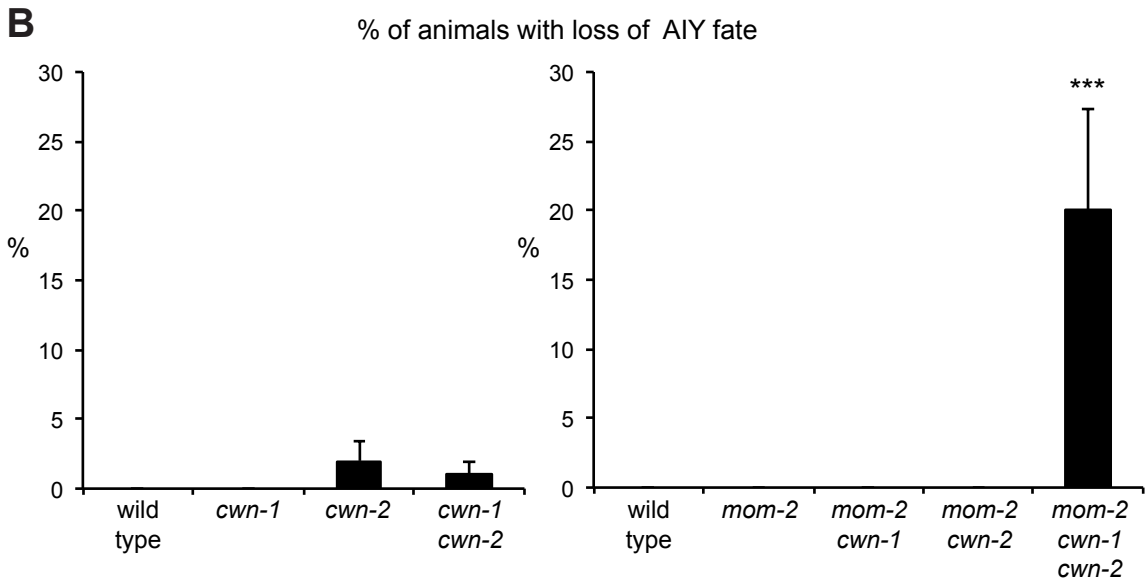
B
% of animals with loss of AIY fate
%
wild type
cwn-1
cwn-2
cwn-1 cwn-2
mom-2
mom-2 cwn-1
mom-2 cwn-2
mom-2 cwn-1 cwn-2
***

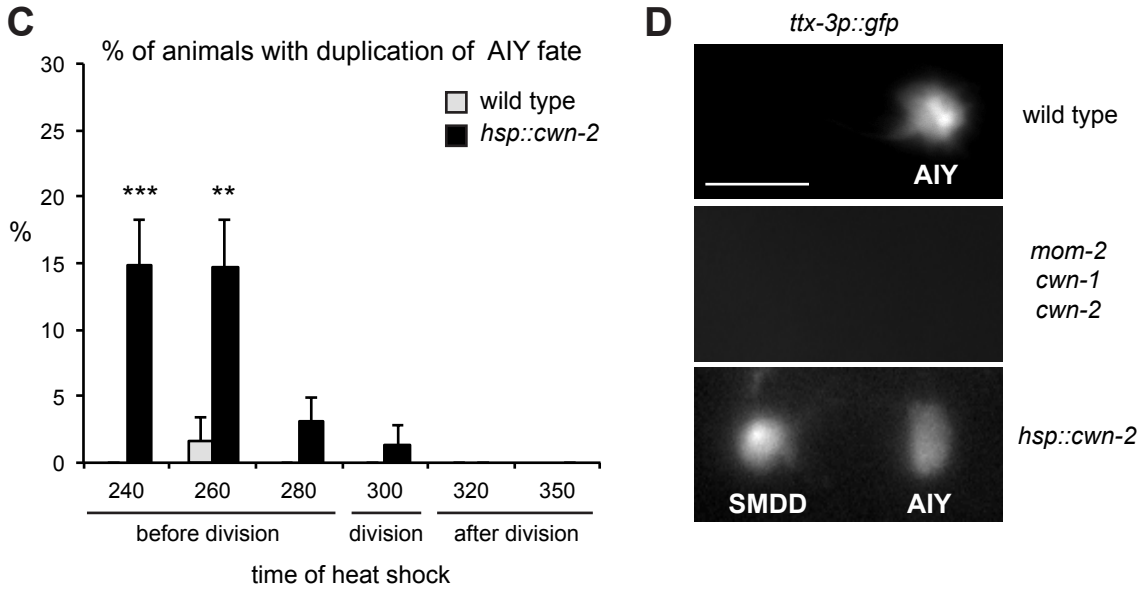
C
% of animals with duplication of AIY fate
wild type
hsp::cwn-2
***
**
%
240
260
280
300
320
350
before division
division
after division
time of heat shock
D
ttx-3p::gfp
AIY
wild type
mom-2 cwn-1 cwn-2
SMDD
AIY
hsp::cwn-2

Figure 2

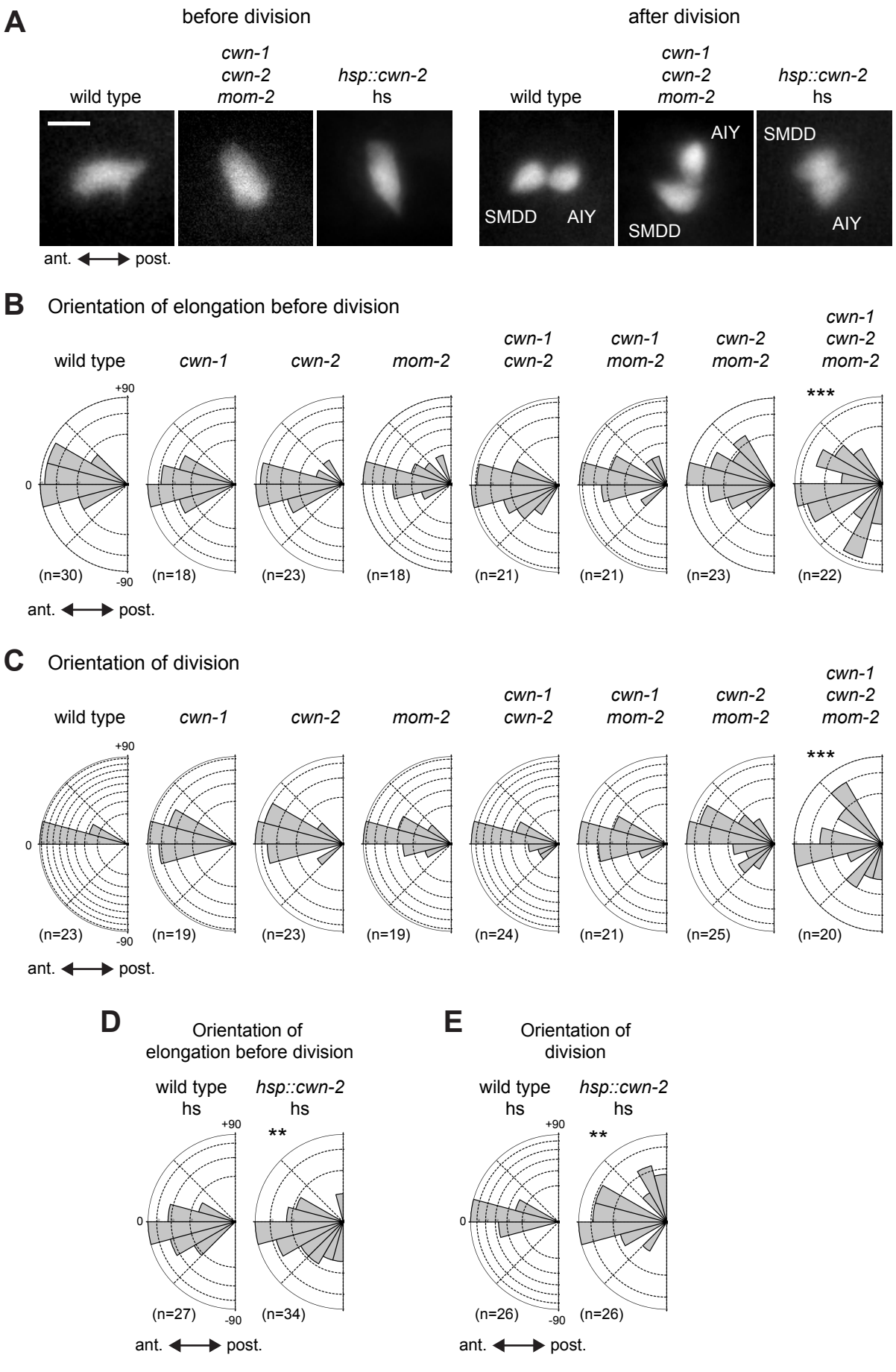
A
before division
after division
wild type
cwn-1
cwn-2
mom-2
hsp::cwn-2
hs
wild type
cwn-1
cwn-2
mom-2
hsp::cwn-2
hs
SMDD
AIY
AIY
SMDD
SMDD
AIY
ant.
post.
B
Orientation of elongation before division
wild type
cwn-1
cwn-2
mom-2
cwn-1
cwn-2
cwn-1
mom-2
cwn-2
mom-2
cwn-1
cwn-2
mom-2
+90
0
-90
***
(n=30)
(n=18)
(n=23)
(n=18)
(n=21)
(n=21)
(n=23)
(n=22)
ant.
post.
C
Orientation of division
wild type
cwn-1
cwn-2
mom-2
cwn-1
cwn-2
cwn-1
mom-2
cwn-2
mom-2
cwn-1
cwn-2
mom-2
+90
0
-90
***
(n=23)
(n=19)
(n=23)
(n=19)
(n=24)
(n=21)
(n=25)
(n=20)
ant.
post.
D
Orientation of elongation before division
wild type
hs
hsp::cwn-2
hs
+90
0
-90
**
(n=27)
(n=34)
ant.
post.
E
Orientation of division
wild type
hs
hsp::cwn-2
hs
+90
0
-90
**
(n=26)
(n=26)
ant.
post.

Figure 3

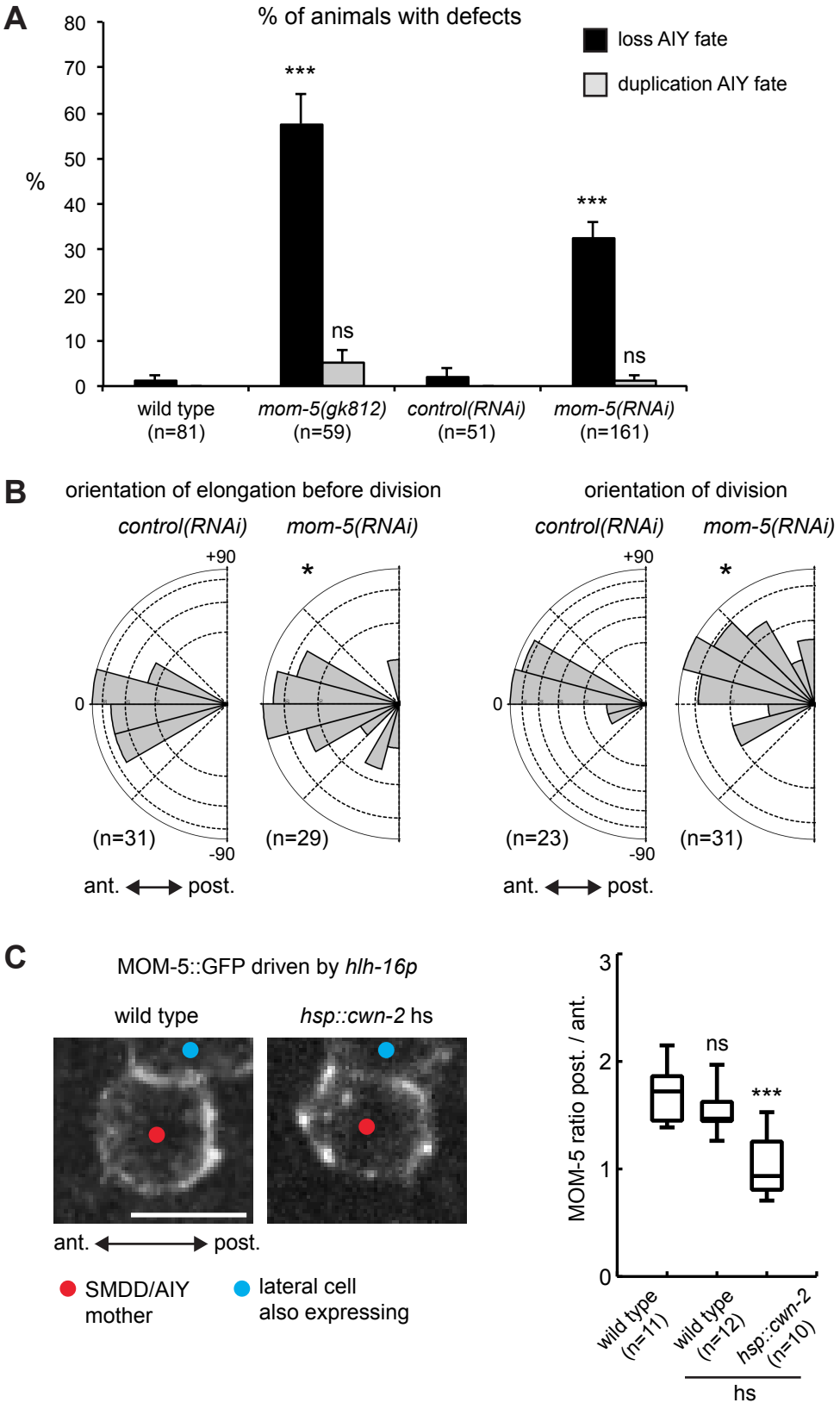
A
% of animals with defects
loss AIY fate
duplication AIY fate
%
80
70
60
50
40
30
20
10
0
***
ns
***
ns
wild type
(n=81)
mom-5(gk812)
(n=59)
control(RNAi)
(n=51)
mom-5(RNAi)
(n=161)
B
orientation of elongation before division
orientation of division
control(RNAi)
mom-5(RNAi)
control(RNAi)
mom-5(RNAi)
+90
-90
0
*
*
(n=31)
(n=29)
(n=23)
(n=31)
ant. post.
ant. post.
C
MOM-5::GFP driven by hlh-16p
wild type
hsp::cwn-2 hs
ant. post.
SMDD/AIY mother
lateral cell also expressing
MOM-5 ratio post. / ant.
3
2
1
0
ns
***
wild type (n=11)
wild type (n=12)
hsp::cwn-2 (n=10)
hs

Figure 4

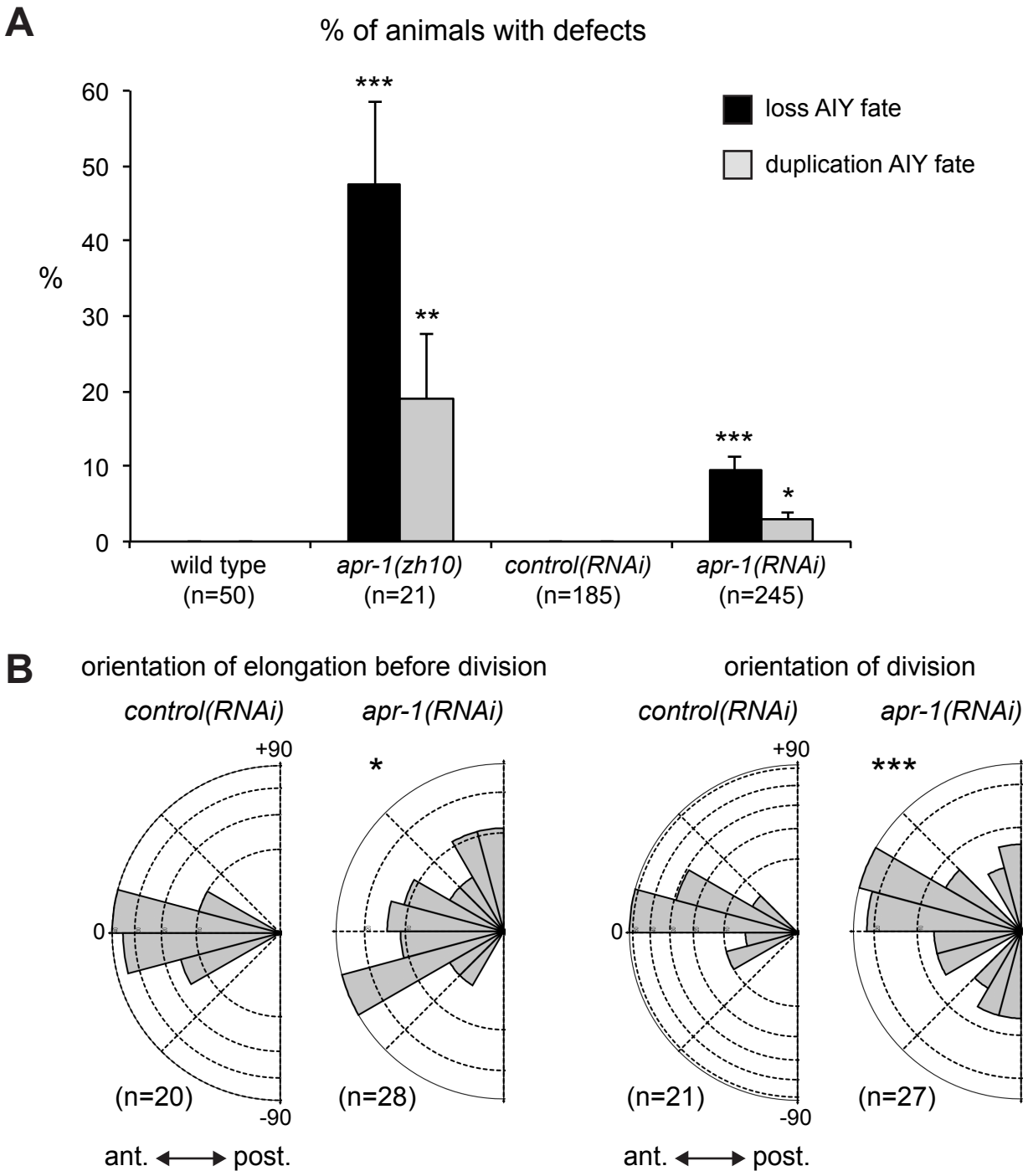
A
% of animals with defects
60
50
40
%
30
20
10
0
***
**
***
*
loss AIY fate
duplication AIY fate
wild type
(n=50)
apr-1(zh10)
(n=21)
control(RNAi)
(n=185)
apr-1(RNAi)
(n=245)
B
orientation of elongation before division
orientation of division
control(RNAi)
apr-1(RNAi)
control(RNAi)
apr-1(RNAi)
+90
0
-90
*
***
(n=20)
(n=28)
(n=21)
(n=27)
ant.
post.
ant.
post.

Figure 5

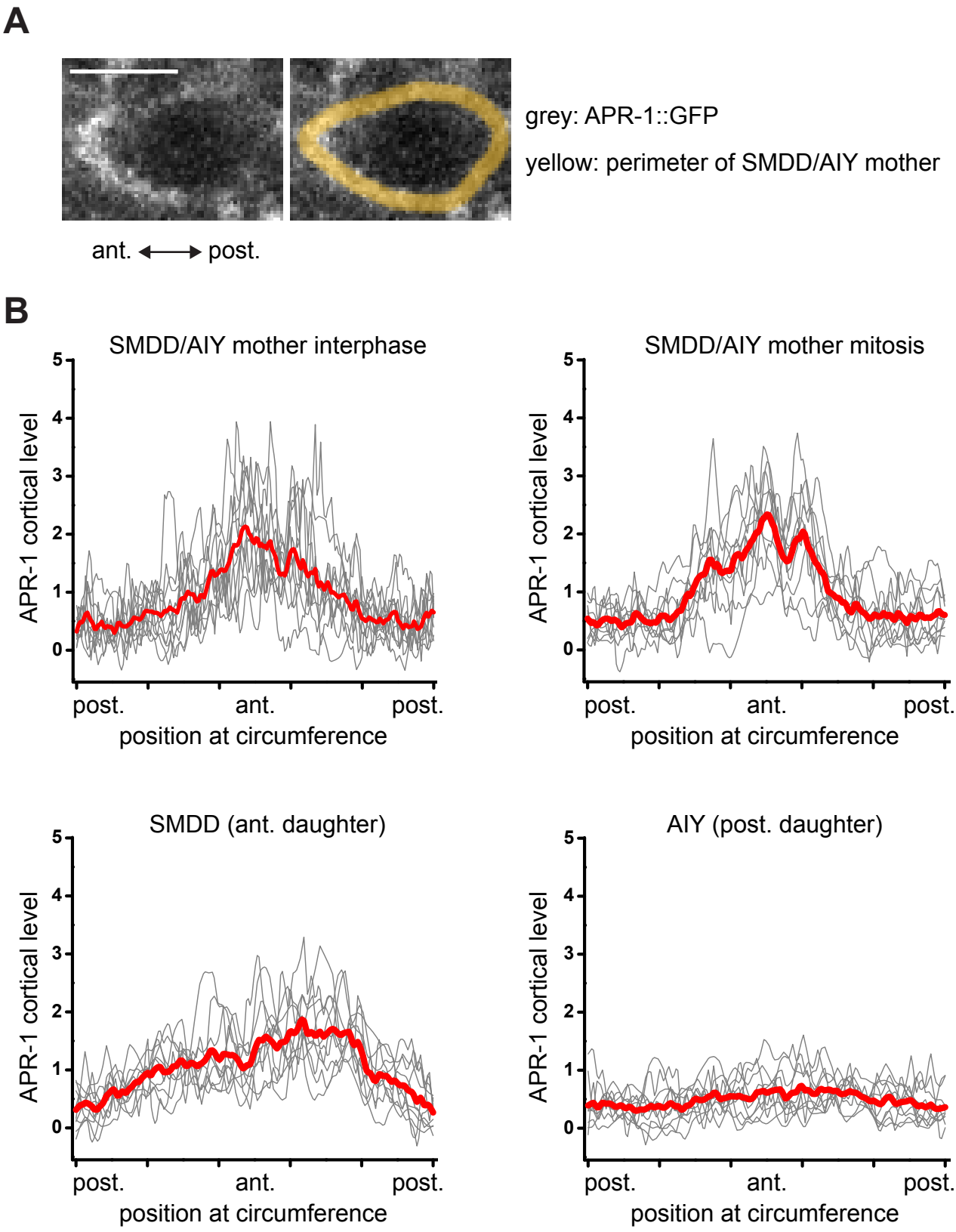
A
grey: APR-1::GFP
yellow: perimeter of SMDD/AIY mother
ant.
post.
B
SMDD/AIY mother interphase
SMDD/AIY mother mitosis
SMDD (ant. daughter)
AIY (post. daughter)
APR-1 cortical level
0
1
2
3
4
5
post.
ant.
post.
position at circumference

Figure 6

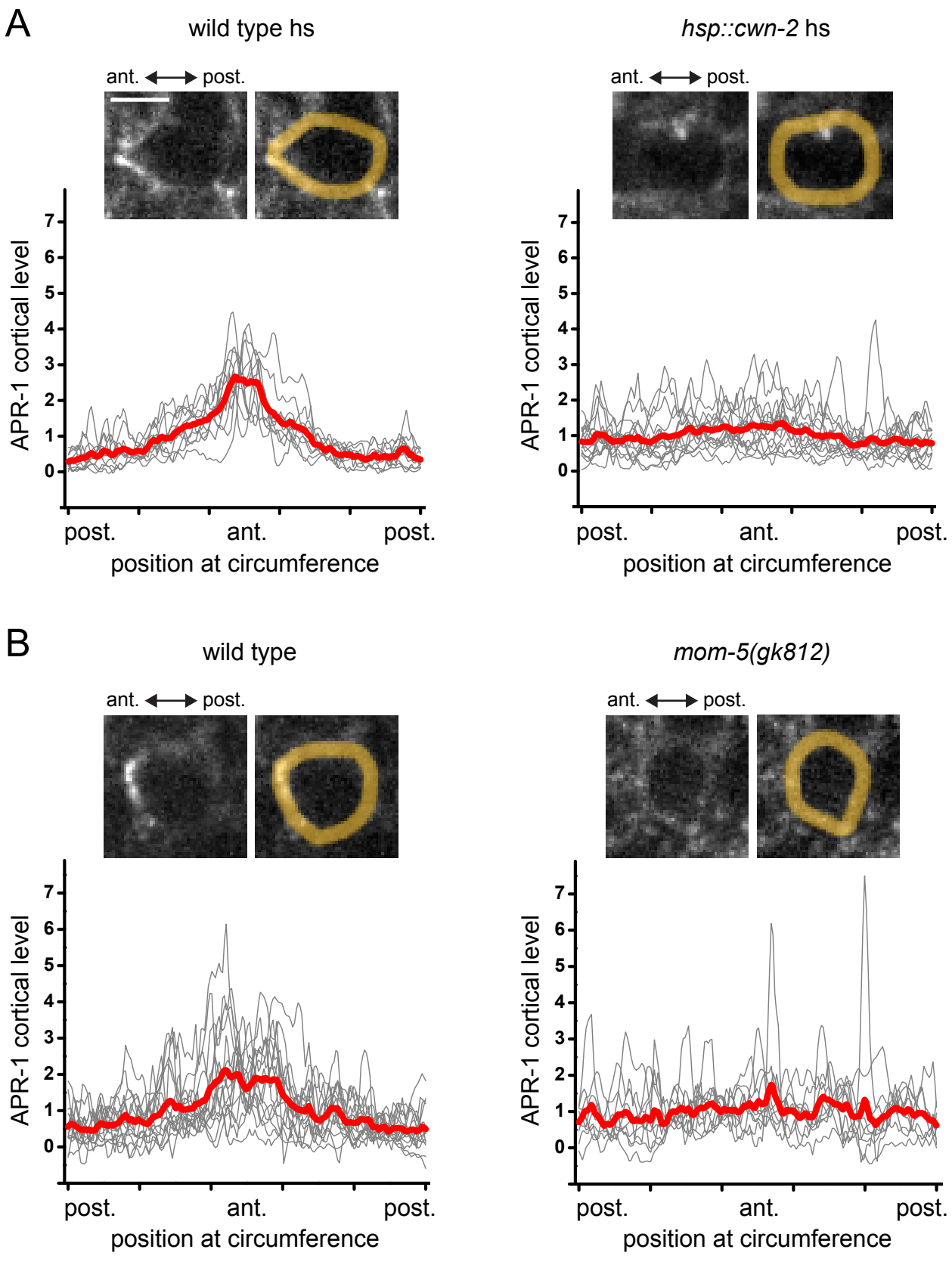
A
wild type hs
hsp::cwn-2 hs
ant. post.
APR-1 cortical level
0
1
2
3
4
5
6
7
post.
ant.
post.
position at circumference
B
wild type
mom-5(gk812)

Figure 7

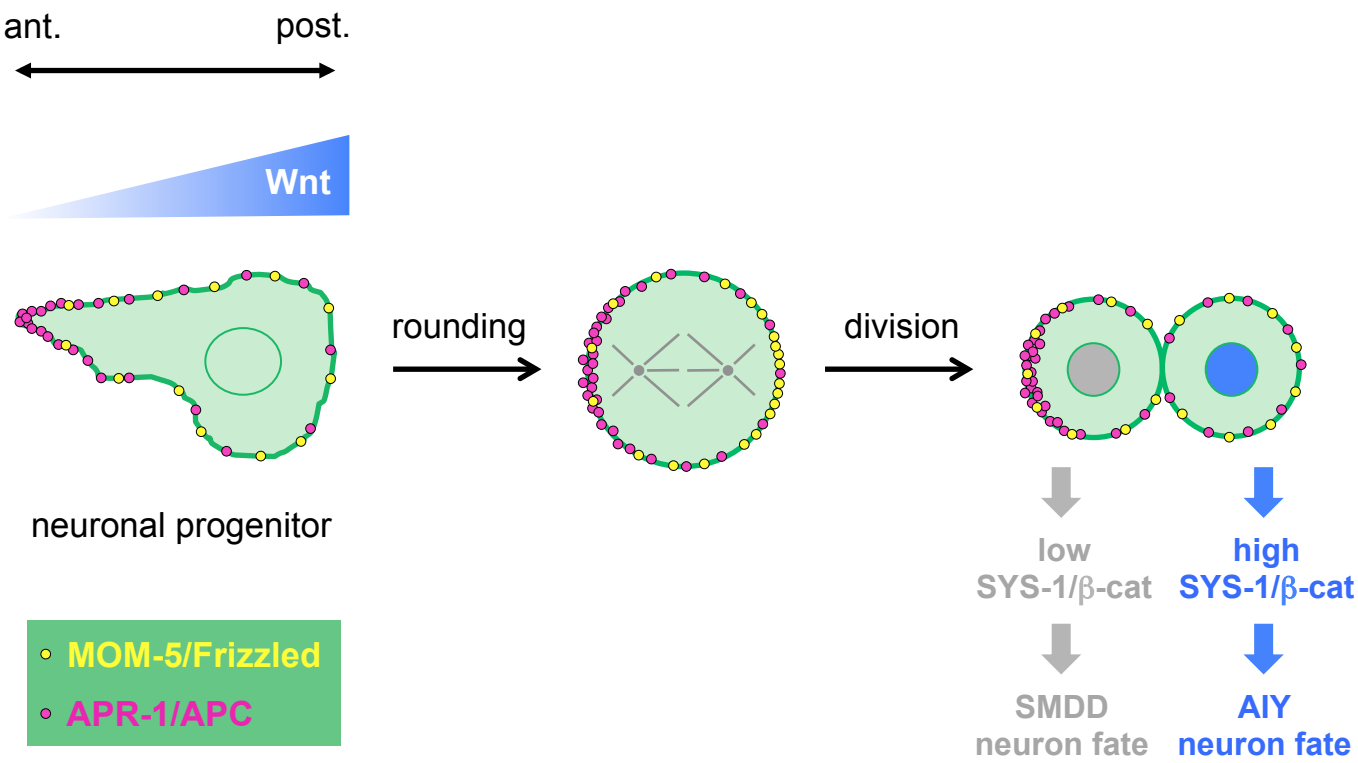
ant.
post.
Wnt
rounding
division
neuronal progenitor
MOM-5/Frizzled
APR-1/APC
low
SYS-1/β-cat
high
SYS-1/β-cat
SMDD
neuron fate
AIY
neuron fate

Figure 8

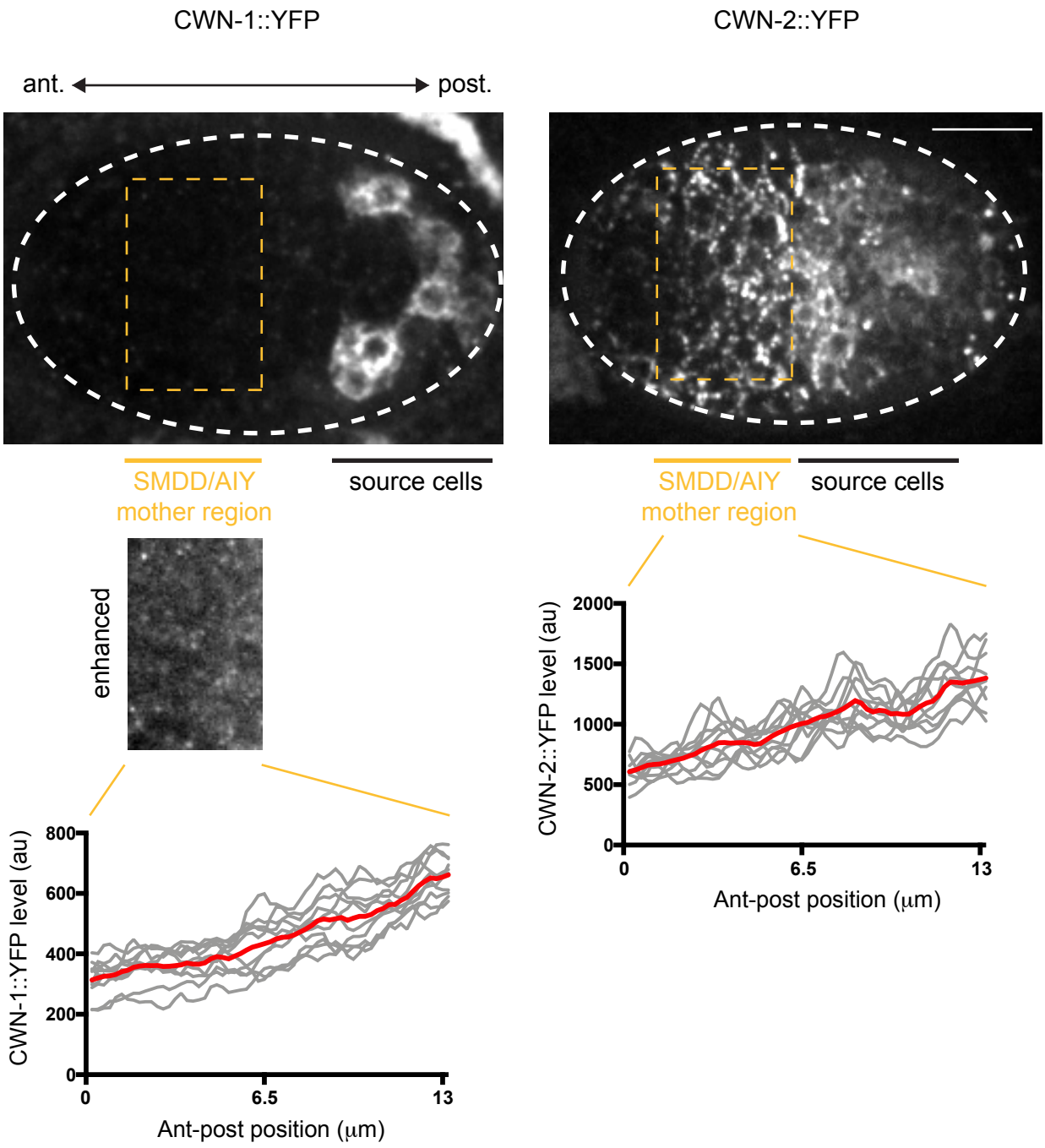

Fig. S1. Expression of CWN-1::YFP and CWN-2::YFP protein fusions. Expression of CWN-1::YFP (*vbaIs38*) and CWN-2::YFP (*vbaIs43*) protein fusions in the embryo at epidermal enclosure stage. Ventral view, scale bar = 10 µm. The orange boxes represent the region where the two SMDD/AIY mothers are located and where the CWN-1::YFP and CWN-2::YFP levels are measured. For CWN-1::YFP a version of the box where fluorescent signal is enhanced is also presented. Graph: CWN-1::YFP and CWN-2::YFP levels in the SMDD/AIY mother region (orange box) plotted along the anteroposterior axis. The grey curves represent individual embryos and the red curve represents the mean curve, n= 10 embryos for each genotype (the maximum anteroposterior elongation observed for the SMDD/AIY mother cell is 10 µm).

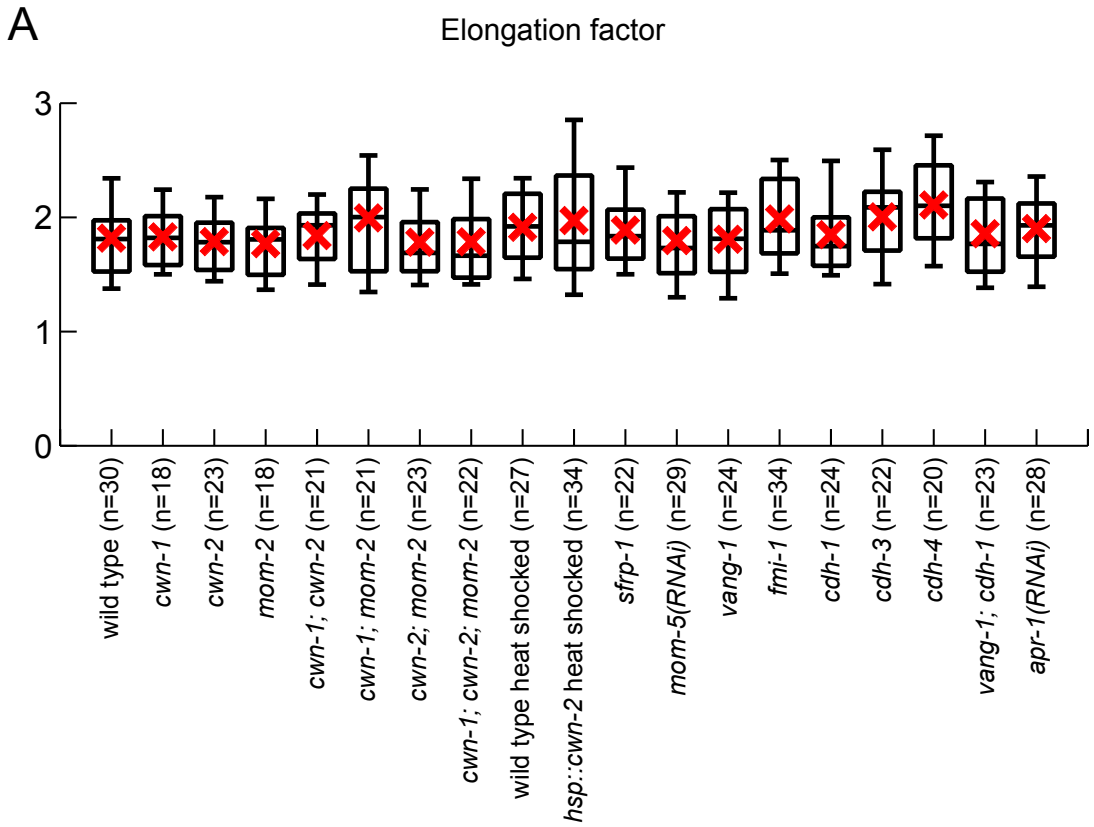

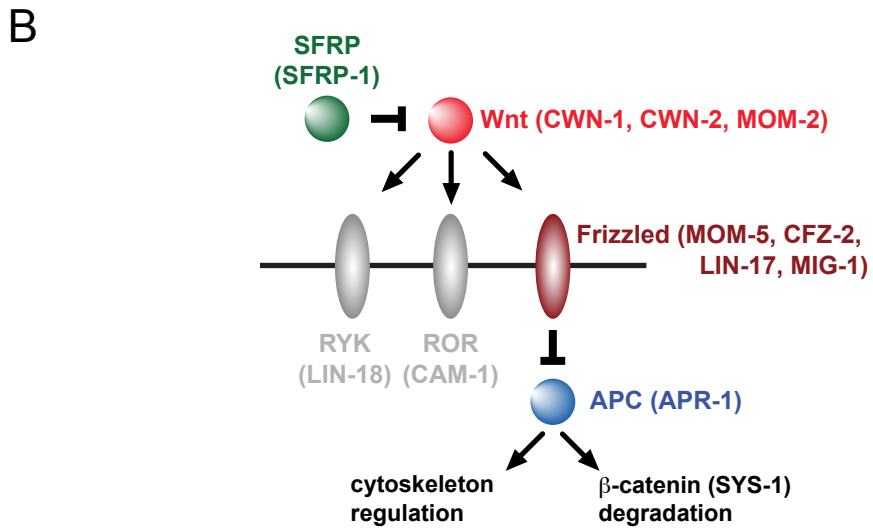

Fig. S2. Effect of various mutants on the elongation factor of the SMDD/AIY mother cell. (A) Elongation factor of the SMDD/AIY mother cell (labeled with *ttx-3p::gfp*) during interphase in various mutant or RNAi treated embryos. The black box represents the median and quartiles; the whiskers represent the 9th and 91st percentiles; the red cross represents the mean; n = number of cells. (B) Scheme of the Wnt pathway presenting the different components analyzed in this study.

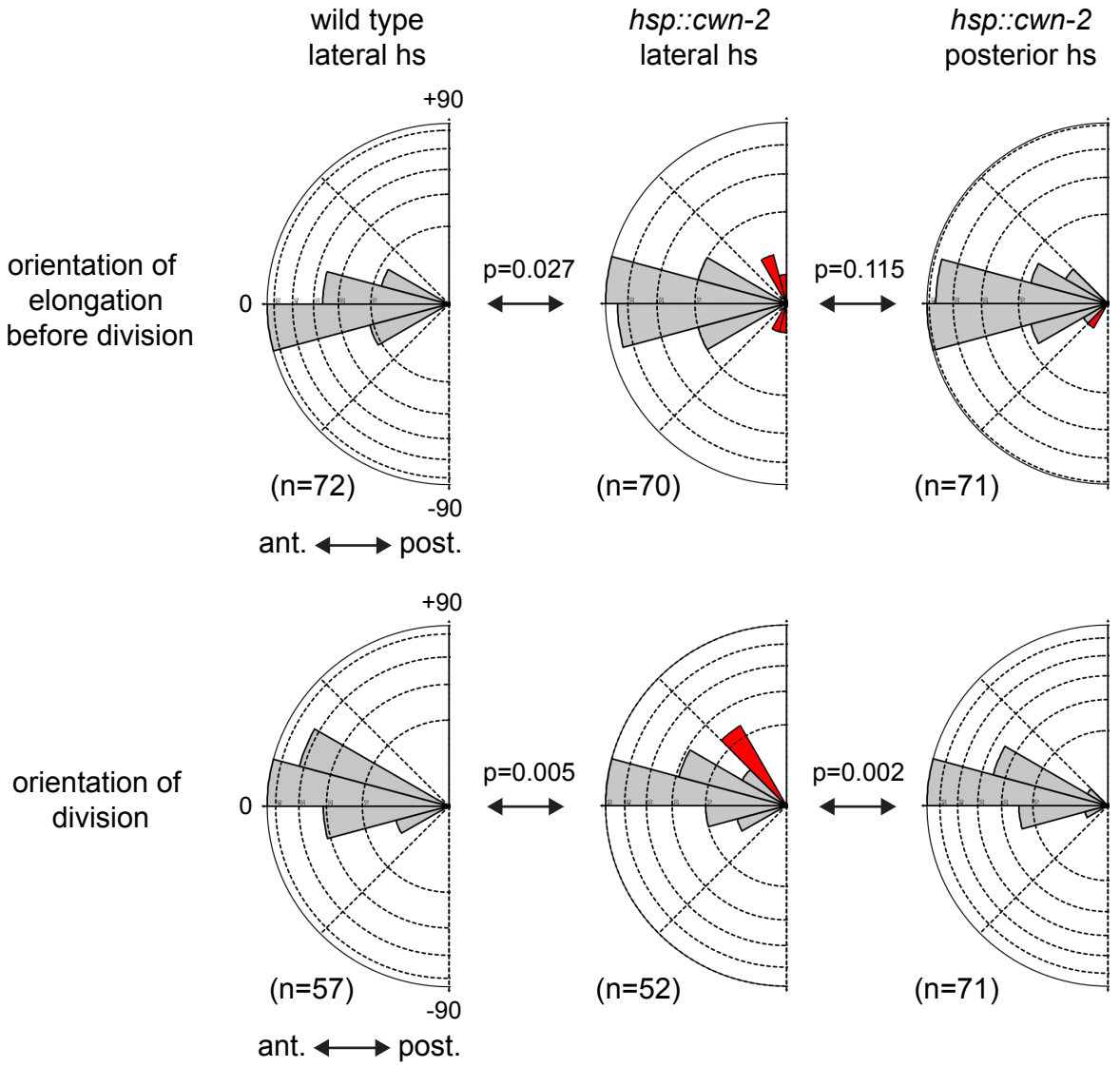

Fig. S3. Induction of a local source of Wnt in the embryo using a laser. Orientation of the elongation of the SMDD/AIY mother (labeled with *ttx-3p::gfp*) before division or of the SMDD/AIY mother division in wild type or *hsp::cwn-2* (*vbaIs5*) embryos. Local heat shock was performed laterally or posteriorly. Rose plot: 0° anterior, -90° lateral, +90° medial, circular grid 10%, n = number of cells, p values Fisher.

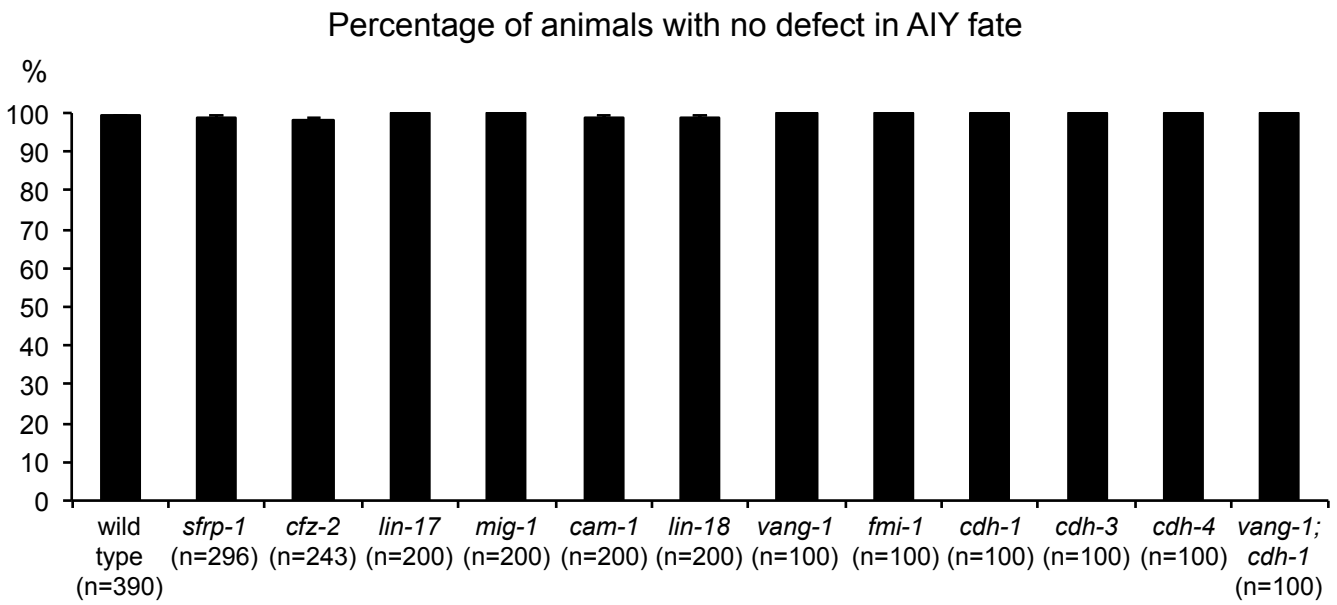

Fig. S4. Effect of various mutants on the fate of the AIY neuron. Percentage of animals presenting a wild type expression of *ttx-3p::gfp* in the two AIY neurons at late larval stage (L4). Error bars = s.e.p., n = number of animals.

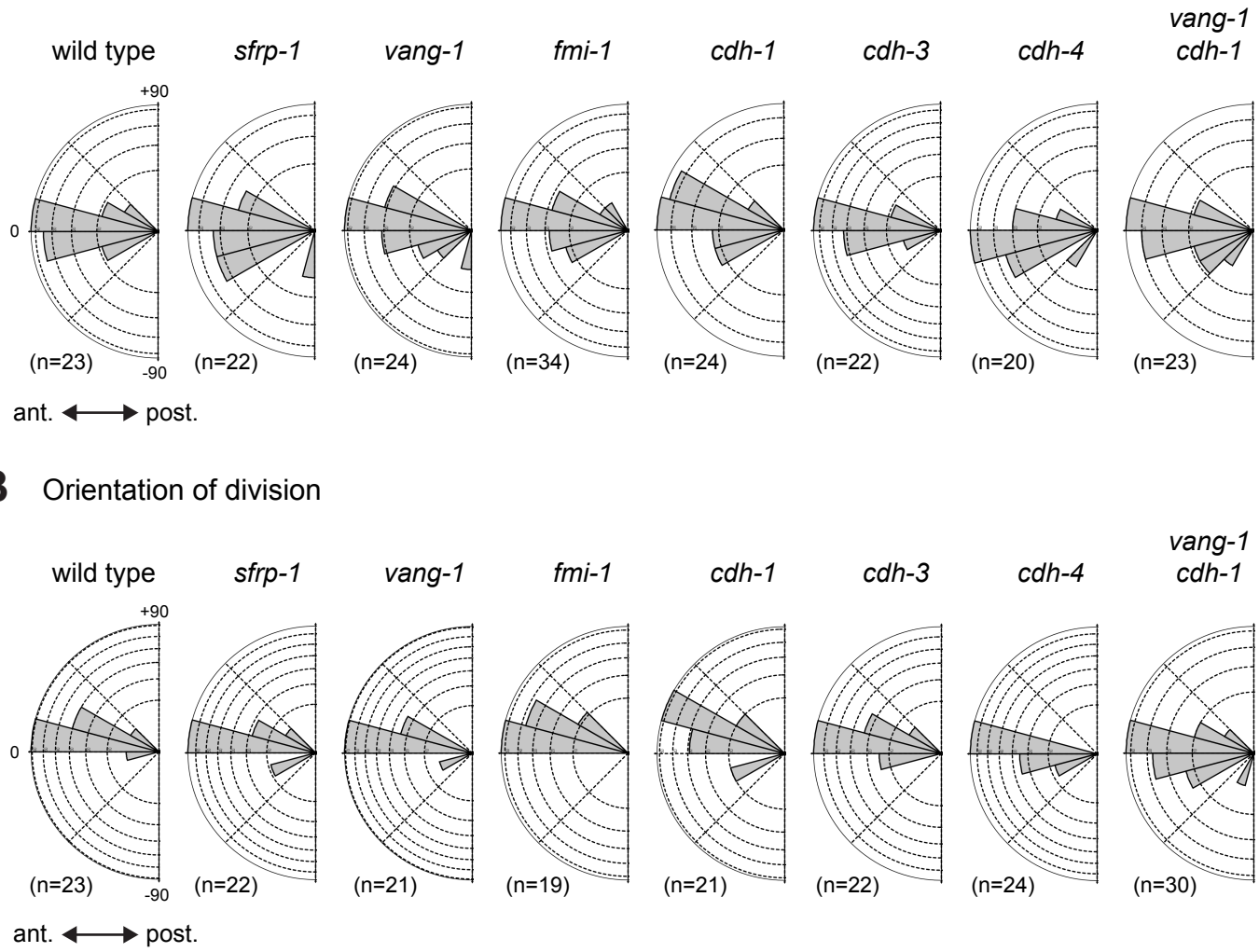

Fig. S5. Effect of various mutants on orientation. (A) Orientation of the elongation of the SMDD/AIY mother cell (marked with *ttx-3p::gfp*) before division. (B) Orientation of the division of the SMDD/AIY mother cell. Rose plot: 0° anterior, -90° lateral, +90° medial, circular grid 10%, n = number of cells.

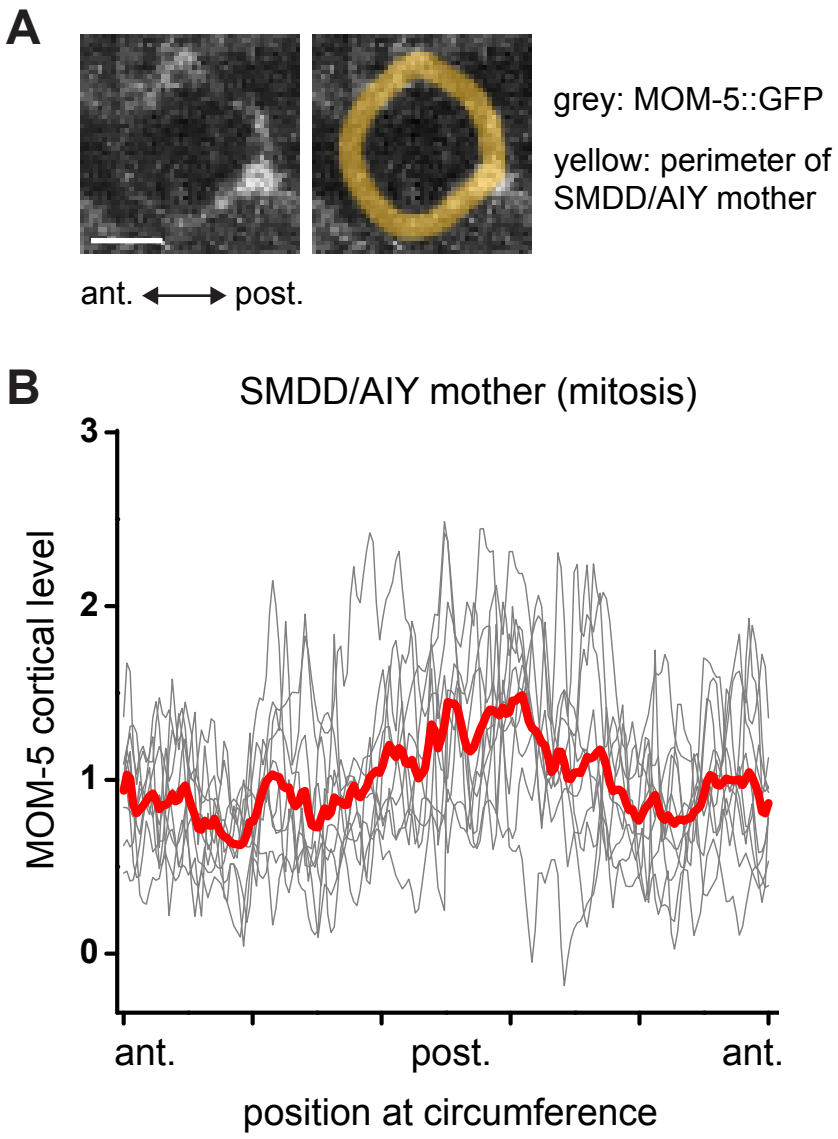

Fig. S6. MOM-5 localization. (A) Localization of MOM-5::GFP (*zuIs145*) in the SMDD/AIY mother cell (identified with *hlh-16p::mCherry*, *otIs10546*) during mitosis (cell rounded). The perimeter of the SMDD/AIY mother cell is indicated in yellow. Ventral view, scale bar = 2 µm. (B) MOM-5::GFP fluorescence intensity profile at the membrane of the SMDD/AIY neuronal progenitor. The x-axis presents the position at the circumference of the cell with the posterior pole in the middle and anterior pole at both ends. The grey curves represent individual cells and the red curve represents the mean curve, n = 10 cells.